A Biomolecular Force Field Based on the Free Enthalpy of Hydration and Solvation: The GROMOS Force-Field Parameter Sets 53A5 and 53A6

CHRIS OOSTENBRINK,[1] ALESSANDRA VILLA,[2] ALAN E. MARK,[2]
WILFRED F. VAN GUNSTEREN[1]
[1]*Laboratory of Physical Chemistry, Swiss Federal Institute of Technology, ETH-Hönggerberg, 8093 Zürich, Switzerland*
[2]*Groningen Biomolecular Sciences and Biotechnology Institute (GBB), Department of Biophysical Chemistry, University of Groningen, Nijenborgh 4, 9747 AG Groningen, The Netherlands*

Received 11 March 2004; Accepted 12 May 2004
DOI 10.1002/jcc.20090
Published online in Wiley InterScience (www.interscience.wiley.com).

Abstract: Successive parameterizations of the GROMOS force field have been used successfully to simulate biomolecular systems over a long period of time. The continuing expansion of computational power with time makes it possible to compute ever more properties for an increasing variety of molecular systems with greater precision. This has led to recurrent parameterizations of the GROMOS force field all aimed at achieving better agreement with experimental data. Here we report the results of the latest, extensive reparameterization of the GROMOS force field. In contrast to the parameterization of other biomolecular force fields, this parameterization of the GROMOS force field is based primarily on reproducing the free enthalpies of hydration and apolar solvation for a range of compounds. This approach was chosen because the relative free enthalpy of solvation between polar and apolar environments is a key property in many biomolecular processes of interest, such as protein folding, biomolecular association, membrane formation, and transport over membranes. The newest parameter sets, 53A5 and 53A6, were optimized by first fitting to reproduce the thermodynamic properties of pure liquids of a range of small polar molecules and the solvation free enthalpies of amino acid analogs in cyclohexane (53A5). The partial charges were then adjusted to reproduce the hydration free enthalpies in water (53A6). Both parameter sets are fully documented, and the differences between these and previous parameter sets are discussed.

 J Comput Chem 25: 1656–1676, 2004

Key words: GROMOS force field; force-field parameterization; free-energy calculation; solvation; hydration

Introduction

Since the 1970s computer simulation has been increasingly used by chemists, physicists, and molecular biologists to gain insight in molecular processes at a resolution often unreachable by experiment. Although any molecular system can in principle be accurately described by quantum mechanics, for most practical applications quantum-mechanical methods remain computationally prohibitively expensive. Alternatively, the Hamiltonian of such a system can be described in terms of classical mechanics by a force field. In classical simulation, the Hamiltonian describing a molecular system can be divided into a kinetic and a potential energy part. The total kinetic energy is simply the sum of the kinetic energies of all the particles constituting the system. The potential energy is, in contrast, a complicated function describing different interactions between these particles.[1,2] Depending on its exact functional form, a force field involves hundreds, if not thousands, of parameters the values of which need to be chosen such that the force field accurately represents the true Hamiltonian.[3–6] Parameterization can be aimed at reproducing properties calculated using higher level theoretical approaches,[4,5,7] or at reproducing chosen experimentally accessible properties.[4,5,8,9]

Correspondence to: W. F. van Gunsteren; e-mail: wfvgn@igc.phys.chem.ethz.ch

Contract/grant sponsor; National Center of Competence in Research (NCCR) Structural Biology of the Swiss National Science Foundation (SNSF).

Received 11 March 2004; Accepted 12 May 2004

Over the past decades a variety of force fields for biomolecular simulations have been developed. An extensive review of force field development, its principles and procedures can be found in ref. 1. Typical examples of condensed phase biomolecular force fields are AMBER,[3,10,11] CHARMM,[4,12,13] CHARMm,[14] ECEPP/3,[15] ENCAD,[16,17] GROMOS,[6,9,18] and OPLS.[5,19] These biomolecular force fields have a similar form of the interaction function, yet they differ considerably in their parameterization philosophy and parameter values. Because the latter can be obtained in a variety of ways, by fitting to a range of molecular properties (geometric, energetic, dynamical, dielectric, etc.) of small molecules against different sets of quantum-mechanical and experimental data regarding these molecules, different parameter sets may yield widely different results when applied to large, complex biomolecular systems.

Since the early 1980s the Groningen Molecular Simulation (GROMOS) software package for computer simulation has been developed in conjunction with an interatomic interaction function for MD simulation of biomolecular systems. Major versions of the GROMOS software are GROMOS87[18] and GROMOS96.[6] The first set of (nonbonded) GROMOS force field parameters can be found in ref. 20. Since then, the force field has continuously been improved and refined.[6,9,18,21–27] The most widely used versions of the GROMOS force field are the GROMOS 37C4 force field[18] of 1985, an improved version[21] of it, the GROMOS 43A1 force field[6,22] of 1996, and the GROMOS 45A3 force field[9] of 2001, see the parameterization section.

All force fields aim at an accurate representation of specific aspects of a physical system. For this reason the question of the general quality of a particular force field cannot be easily answered. It will depend on the type of property and the molecular system under investigation. An impression can, however, be obtained from the literature concerning the application of a particular force field to biomolecular systems for which ample experimental data at the atomic level is available, for example, from NMR spectroscopy or X-ray diffraction. Over the years, the successive GROMOS force-field parameter sets have been tested in simulations of a wide variety of proteins, nucleotides, sugars, and lipids. The most recent tests of the 43A1 parameter set involve a series of β-peptides,[28–31] the proteins fatty acid binding protein,[32] hen egg white lysozyme,[21,33,34] α-lactalbumin,[35,36] photoactive yellow protein,[37] the estrogen receptor ligand-binding domain[38] and DNA duplexes.[39,40] For a review of validation procedures we refer to ref. 41.

The basic philosophy underlying the GROMOS force field is the desire to strike a balance between an accurate description of the interaction energy as function of conformation on the one hand, and a relatively simple functional form on the other. A simple functional form is desirable to minimize the number of parameters required, which facilitates the transfer of parameters between similar moieties, and to limit the computational cost of evaluating the potential energy. Accurate parameters to describe the so-called bonded interactions, as a function of bond lengths, bond angles, and torsional angles can be readily obtained from crystallographic and spectroscopic data for small molecules. The nonbonded interactions, however, which involve electrostatic and van der Waals interactions between (in principle) all pairs of atoms in the system are much more difficult to parameterize. Early values of the GROMOS nonbonded interaction parameters were obtained from crystallographic data and atomic polarizabilities, and adjusted such that experimental distances and interaction energies of individual pairs of functional groups of atoms were reproduced for minimum energy configurations.[20] As computer power increased, it became feasible to use statistical-mechanical approaches to parameterize the nonbonded interactions, for example, by reproducing thermodynamic properties such as the density and the heat of vaporization of small molecules in the condensed phase at physiological temperatures and pressures. The interaction parameters for a number of solvents (water,[42,43] chloroform,[44] methanol,[45] dimethyl sulfoxide,[46,47] carbon tetrachloride[48]) and other relevant small molecules[22] have been obtained in this way. In addition, experimental and *ab initio* quantum-chemical data were used to tune, for instance, the distribution of torsional-angle values around specific bonds.[24,49] Unfortunately, this approach yields mainly information about the interactions of certain functional groups with themselves. It does not necessarily ensure an accurate description of the interaction of the specific group in question with other parts of the force field, which must be inferred, for example, through the use of combination rules for nonbonded parameters.[1]

The continued increase in computational power and in the accuracy of methods to calculate relative free energies has progressively allowed the inclusion of solvation free enthalpies in the parameterization procedure. This procedure was previously applied to alkanes[9,22] to obtain nonpolar atom parameters. Here we extend this approach to include polar compounds. So far, none of the other force fields commonly used in biomolecular simulation (AMBER,[3,10,11] CHARMM,[4,12,13] OPLS[5,19]) have been parameterized against free enthalpies of solvation, only the GROMOS parameters for aliphatic carbon atoms were obtained in this way. However, solvation effects and partition properties play a vital role in most biomolecular processes of interest, such as folding of proteins, recognition, and association of biomolecules, formation of micelles, and membranes, and transport of molecules across membranes. Recently, free enthalpies of solvation have been calculated for neutral amino acid side chains, using the GROMOS, CHARMM, AMBER, and OPLS force fields.[50–52] All of the previously published versions of these force fields seem to strongly underestimate the free enthalpies of hydration for polar compounds, a defect that prompted the current reparameterization of the GROMOS force field as described below. An additional aim of the reparameterization of the GROMOS force field was to obtain a single force field that can be used both for protein and for membrane simulations. Such a force field should not only reproduce interactions between similar atomic moieties, but also partition properties between different media. The combination of this new parameterization with selected previous additions and minor changes to the GROMOS force field[27,49,53–55] has led to the definition of two new parameter sets, 53A5 and 53A6.

The previous parameter sets of the GROMOS force field have always been publicly available. The functional form has also been described earlier.[23,56] Nevertheless, a complete description of the force field, including the parameters and technical details, has so far only been published in the manuals of the GROMOS program.[6,18] Here, we present a complete overview of the functional form of the GROMOS force field and its current parameters, followed by a description of the current reparameterization. This

will ease the use of this latest GROMOS parameterization, because in the 53A5 and 53A6 parameter sets many interactions types have been redefined, and all types have been renumbered with respect to the previous parameter sets.

Functional Form

In a classical molecular dynamics simulation, all degrees of freedom that are treated explicitly are propagated in time according to the appropriate physical laws. For this one needs a description of the Hamiltonian of the system, comprising all energy contributions in which these degrees of freedom take part. In the GROMOS force field a molecular system is treated at an atomic level; every atom has three degrees of freedom and the associated conjugate momenta. Note that in the GROMOS force field aliphatic carbon atoms are treated as united atoms, that is, the carbon and the hydrogens that are bonded to it are treated as a single atom, thus reducing the degrees of freedom that are explicitly simulated. This yields a reduction of computational effort up to a factor of 9 (e.g., for saturated lipids) at the expense of neglecting the slight directional and volume effects of the presence of these hydrogens.

The Hamiltonian that describes such a system can be divided into a kinetic and a potential energy part,

$$H(\mathbf{p}, \mathbf{r}; m, s) = K(\mathbf{p}; m) + V(\mathbf{r}; s). \quad (1)$$

The kinetic energy part is normally independent of the atom coordinates, $\mathbf{r}$, and only a function of the momenta, $\mathbf{p}$, and the masses, m, of the N atoms in the system,

$$K(\mathbf{p}; m) = \sum_{i=1}^{N} \frac{\mathbf{p}_i^2}{2m_i} = \sum_{i=1}^{N} \frac{1}{2} m_i \mathbf{v}_i^2, \quad (2)$$

where $\mathbf{p}_i \equiv m_i \mathbf{v}_i$, and $\mathbf{v}_i$ is the velocity of atom i. In the GROMOS force field, the masses are described by mass atom types, as specified in Table 1.[57] The potential energy term describes the interaction energy between the atoms in terms of the atom coordinates, $\mathbf{r}$, and the force-field parameters, s. To perform a molecular dynamics simulation, one needs to calculate forces on atoms rather than the potential energies. The force, $\mathbf{f}_i$, on an atom i is the negative derivative of the potential energy with respect to atom coordinates $\mathbf{r}_i$,

$$\mathbf{f}_i = -\frac{\partial}{\partial \mathbf{r}_i} V(\mathbf{r}_1, \mathbf{r}_2, \ldots, \mathbf{r}_N; s). \quad (3)$$

The potential energy is usually written as a sum over different contributions, which can correspond to physical atomic interactions or to (special) unphysical interactions that one might want to apply,

$$V(\mathbf{r}; s) = V^{\text{phys}}(\mathbf{r}; s) + V^{\text{special}}(\mathbf{r}; s). \quad (4)$$

V^{special} includes, among others, interactions that are added to restrain a certain property in the course of a simulation (position, distance, dihedral angle restraining).[6] Here they will not be considered any further, we will limit ourselves to the physical interaction energies. These can again be divided into bonded and nonbonded interactions,

$$V^{\text{phys}}(\mathbf{r}; s) = V^{\text{bon}}(\mathbf{r}; s) + V^{\text{nbon}}(\mathbf{r}; s). \quad (5)$$

In the GROMOS force field the bonded interactions are the sum of bond, bond angle, harmonic (improper) dihedral angle, and trigonometric (torsional) dihedral angle terms. The nonbonded interactions are the sum of van der Waals (Lennard–Jones, LJ) and electrostatic (Coulomb with Reaction Field, CRF) interactions between (in principle) all pairs of atoms,

$$V^{\text{bon}}(\mathbf{r}; s) = V^{\text{bond}}(\mathbf{r}; s) + V^{\text{angle}}(\mathbf{r}; s) + V^{\text{har}}(\mathbf{r}; s) + V^{\text{trig}}(\mathbf{r}; s) \quad (6)$$

$$V^{\text{nbon}}(\mathbf{r}; s) = V^{\text{LJ}}(\mathbf{r}; s) + V^{\text{CRF}}(\mathbf{r}; s). \quad (7)$$

All individual terms in eqs. (6) and (7) will be described separately in the following subsections.

Covalent Bond Interactions

In the current version of the GROMOS force field the potential energy due to covalent bond interactions is calculated as the sum over all N_b bonds and depends on the parameters K_b and b_0,

$$V^{\text{bond}}(\mathbf{r}; s) = V^{\text{bond}}(\mathbf{r}; K_b, b_0) = \sum_{n=1}^{N_b} \frac{1}{4} K_{b_n} [b_n^2 - b_{0_n}^2]^2. \quad (8)$$

Table 1. The GROMOS Force-Field Parameter Sets 53A5 and 53A6.

Mass Atom Type Code	Mass in a.m.u.[a]	Mass Atom Name
1	1.008	H
3	13.019	CH1
4	14.027	CH2
5	15.035	CH3
6	16.043	CH4
12	12.011	C
14	14.0067	N
16	15.9994	O
19	18.9984	F
23	22.9898	NA
24	24.305	MG
28	28.08	SI
31	30.9738	P
32	32.06	S
35	35.453	CL
39	39.948	AR
40	40.08	CA
56	55.847	FE
63	63.546	CU
65	65.37	ZN
80	79.904	BR

[a]Taken from ref. 57.

The actual bond length for the nth bond between atoms i and j with positions $\mathbf{r}_i$ and $\mathbf{r}_j$ is given by $b_n = r_{ij} = \sqrt{\mathbf{r}_{ij} \cdot \mathbf{r}_{ij}}$ where $\mathbf{r}_{ij} = \mathbf{r}_i - \mathbf{r}_j$. The parameters K_b and b_0 are defined over the GROMOS bond types, which are specified together with the parameter values in Table 2. These have originally been derived from experimental spectroscopic (K_b) and X-ray diffraction (b_0) data for small molecules.[58,59]

The functional form of eq. (8) is anharmonic. It was chosen for computational reasons, reducing the number of square-root operations in the evaluation of the interaction energy and forces. In the physically realistic range of bond lengths, the potential energies are essentially indistinguishable. The corresponding harmonic bond constant can be calculated from K_{b_n} and b_{0_n} as $K_{b_n}^{\text{harm}} = 2K_{b_n}b_{0_n}^2$.

Covalent Bond-Angle Interactions

As for the bonds, the potential energy due to covalent bond-angle interactions is calculated as the sum over all N_θ bond angles and depends on the parameters K_θ and θ_0,

$$V^{\text{angle}}(\mathbf{r}; s) = V^{\text{angle}}(\mathbf{r}; K_\theta, \theta_0) = \sum_{n=1}^{N_\theta} \frac{1}{2} K_{\theta_n}[\cos\theta_n - \cos\theta_{0_n}]^2. \quad (9)$$

with θ_n being the actual value of the nth angle defined by atoms i, j, k. K_θ, and θ_0 are defined over bond-angle types that are together with the parameter values specified in Table 3. These have originally been derived from experimental spectroscopic (K_θ) and X-ray diffraction (θ_0) data for small molecules.[58,59]

This functional form has been chosen for computational reasons rather than a more commonly used expression, which is purely harmonic in θ_n. In the GROMOS form only the value and derivative of cos θ_n is needed, which saves an arccosine operation. In addition, this functional form has the advantage of numerical stability as θ_n approaches 180°, whereas an interaction that is harmonic in θ_n, results in a singularity in the force for $\theta_n = 180°$. The force constant K_{θ_n} can be related to a corresponding harmonic force constant $K_{\theta_n}^{\text{harm}}$ (>0) by requiring that the energies of both forms are equal to k_BT for the same deviations $\pm(\theta - \theta_0)$ from the ideal angle θ_0. So,

$$K_{\theta_n} = \frac{2k_BT}{[\cos(\theta_{0_n} + \sqrt{k_BT/K_{\theta_n}^{\text{harm}}}) - \cos\theta_{0_n}]^2 + [\cos(\theta_{0_n} - \sqrt{k_BT/K_{\theta_n}^{\text{harm}}}) - \cos\theta_{0_n}]^2} \quad (10)$$

where k_B is the Boltzmann constant ($8.31441 \cdot 10^{-3}$ kJ/mol) and T the temperature, which is usually taken to be 300 K when applying this equation.

Improper Dihedral-Angle Interactions

Improper dihedral-angle interactions (also called harmonic, out-of-plane, or out-of-tetrahedral dihedral-angle interaction) are used to keep a set of four atoms in a specific configuration. Examples are keeping four atoms in a plane, or maintaining a tetrahedral configuration around a sp3 hybridized carbon atom of which only three bound neighbor atoms are treated explicitly (i.e., a united CH atom). The potential energy due to these interactions is again calculated as a sum over N_ξ improper dihedral interaction centers, with parameters K_ξ and ξ_0,

$$V^{\text{har}}(\mathbf{r}; s) = V^{\text{har}}(\mathbf{r}; K_\xi, \xi_0) = \sum_{n=1}^{N_\xi} \frac{1}{2} K_{\xi_n}[\xi_n - \xi_{0_n}]^2, \quad (11)$$

with ξ_n being the actual value of a dihedral angle defined by atoms i, j, k, and l. This angle can be calculated from the atomic positions, $\mathbf{r}$, as

$$\xi_n = \text{sign}(\xi_n)\arccos\left(\frac{\mathbf{r}_{mj} \cdot \mathbf{r}_{qk}}{r_{mj}r_{qk}}\right), \quad (12)$$

where $\mathbf{r}_{mj} \equiv \mathbf{r}_{ij} \times \mathbf{r}_{kj}$, $\mathbf{r}_{qk} \equiv \mathbf{r}_{kj} \times \mathbf{r}_{kl}$ with the indices m and q defined through the cross products and the sign of the angle ξ_n is given by $\text{sign}(\xi_n) = \text{sign}(\mathbf{r}_{ij} \cdot \mathbf{r}_{qk})$. The angle ξ_n is not defined if $r_{mj} = 0$ or $r_{qk} = 0$. Because $0 \leq \arccos \leq \pi$, we get $-\pi \leq \xi_n \leq \pi$, forcing us to take the argument $[\xi_n - \xi_{0_n}]$ in eq. (11) modulo 2π.

In the GROMOS force field the parameters K_ξ and ξ_0 for improper dihedral angles are defined over improper dihedral-angle types, which are together with the parameter values specified in Table 4. Only three types are distinguished—one tetrahedral type and two planar ones with different force constants.

Torsional Dihedral-Angle Interactions

Proper torsional dihedral-angles are treated using a trigonometric function. The total potential energy coming from torsional interactions is calculated as a sum over N_φ torsional dihedral angles, using the parameters K_φ, δ, and m,

$$V^{\text{trig}}(\mathbf{r}; s) = V^{\text{trig}}(\mathbf{r}; K_\varphi, \delta, m) = \sum_{n=1}^{N_\varphi} K_{\varphi_n}[1 + \cos(\delta_n)\cos(m_n\varphi_n)], \quad (13)$$

where δ_n is the phase shift, which is restricted to 0 or π (i.e., cos $\delta_n = \pm 1.0$), m_n is the multiplicity of the torsional dihedral angle and φ_n is the actual value of the dihedral angle defined by atoms i, j, k, and l. It can in principle be calculated using eq. (12), but because of the trigonometric functional form, the arccos operation can be avoided. The $\cos(m_n\varphi_n)$ terms are written explicitly as polynomials in $\cos(\varphi_n)$ up to multiplicities of 6.

Table 2. Bond-Stretching Parameters.

Bond type code I	Parameters for type I: Force constant K_b (10^6kJmol^{-1}nm^{-4})	Parameters for type I: Ideal bond length b_0 (nm)	Examples of usage in terms of nonbonded atom types
1	15.7	0.100	H—OA
2	18.7	0.100	H—N (all)
3	12.3	0.109	HC—C
4	37.0	0.112	C—O (CO bound to heme)
5	16.6	0.123	C—O
6	13.4	0.125	C—OM
7	12.0	0.132	CR1—NR (6-ring)
8	8.87	0.133	H—S
9	10.6	0.133	C—NT, NL
10	11.8	0.133	C, CR1—N, NR, CR1, C (peptide, 5-ring)
11	10.5	0.134	C—N, NZ, NE
12	11.7	0.134	C—NR (no H) (6-ring)
13	10.2	0.136	C—OA, FTfe—CTfe
14	11.0	0.138	C—NR (heme)
15	8.66	0.139	CH2—C, CR1 (6-ring)
16	10.8	0.139	C, CR1—CH2, C, CR1 (6-ring)
17	8.54	0.140	C, CR1, CH2—NR (6-ring)
18	8.18	0.143	CHn—OA
19	9.21	0.143	CHn—OM
20	6.10	0.1435	CHn—OA (sugar)
21	8.71	0.147	CHn—N, NT, NL, NZ, NE
22	5.73	0.148	CHn—NR (5-ring)
23	7.64	0.148	CHn—NR (6-ring)
24	8.60	0.148	O, OM—P
25	8.37	0.150	O—S
26	5.43	0.152	CHn—CHn (sugar)
27	7.15	0.153	C, CHn—C, CHn
28	4.84	0.161	OA—P
29	4.72	0.163	OA—SI
30	2.72	0.178	FE—C (CO bound to heme)
31	5.94	0.178	CH3—S
32	5.62	0.183	CH2—S
33	3.59	0.187	CH1—SI
34	0.640	0.198	NR (His)—FE (43A1)
35	0.628	0.200	NR (heme)—FE
36	5.03	0.204	S—S
37	0.540	0.221	NR (His)—FE
38	23.2	0.100	HWat—OWat
39	12.1	0.110	HChl—CChl
40	8.12	0.1758	CChl—CLChl
41	8.04	0.153	ODmso—SDmso
42	4.95	0.193799	SDmso—CDmso
43	8.10	0.176	CCl4—CLCl4
44	13.1	0.1265	CUrea—OUrea
45	10.3	0.135	CUrea—NUrea
46	8.71	0.163299	HWat—HWat
47	2.68	0.233839	HChl—CLChl
48	2.98	0.290283	CLChl—CLChl
49	2.39	0.279388	ODmso—CDmso
50	2.19	0.291189	CDmso—CDmso
51	3.97	0.2077	HMet—CMet
52	3.04	0.287407	CLCl4—CLCl4

Bond types currently available in the 53A5 and 53A6 parameter sets. The atom names in the last column correspond to the atom types that are defined in Table 6. Parameters for (co)solvents (bond types 38–52) have often been parameterized to a higher accuracy, and are therefore presented here using a larger number of significant digits.

Table 3. Bond-Angle Bending Parameters.

Bond-angle type code I	Parameters for type I: Force constant K_θ (kJmol^{-1})	Parameters for type I: Ideal bond angle θ_0 (degree)	Examples of usage in terms of nonbonded atom types
1	380	90.0	NR (heme)—FE—C (CO bound to heme)
2	420	90.0	NR (heme)—FE—NR (heme), NR (His)
3	405	96.0	H—S—CH2
4	475	100.0	CH2—S—CH3
5	420	103.0	OA—P—OA
6	490	104.0	CH2—S—S
7	465	108.0	NR, C, CR1 (5-ring)
8	285	109.5	CHn—CHn—CHn, NR (6-ring) (sugar)
9	320	109.5	CHn, OA—CHn—OA, NR (ring) (sugar)
10	380	109.5	H—NL, NT—H, CHn—OA—CHn (sugar)
11	425	109.5	H—NL—C, CHn H—NT—CHn
12	450	109.5	X—OA, SI—X
13	520	109.5	CHn, C—CHn—C, CHn, OA, OM, N, NE
14	450	109.6	OM—P—OA
15	530	111.0	CHn—CHn—C, CHn, OA, NR, NT, NL
16	545	113.0	CHn—CH2—S
17	50.0	115.0	NR (heme)—FE—NR (His) (43A1)
18	460	115.0	H—N—CHn
19	610	115.0	CHn, C—C—OA, N, NT, NL
20	465	116.0	H—NE—CH2
21	620	116.0	CH2—N—CH1
22	635	117.0	CH3—N—C, CHn—C—OM
23	390	120.0	H—NT, NZ, NE—C
24	445	120.0	H—NT, NZ—H
25	505	120.0	H—N—CH3, H, HC—6-ring, H—NT—CHn
26	530	120.0	P, SI—OA—CHn, P
27	560	120.0	N, C, CR1 (6-ring, no H)
28	670	120.0	NZ—C—NZ, NE
29	780	120.0	OM—P—OM
30	685	121.0	O—C—CHn, C CH3—N—CHn
31	700	122.0	CH1, CH2—N—C
32	415	123.0	H—N—C
33	730	124.0	O—C—OA, N, NT, NL C—NE—CH2
34	375	125.0	FE—NR—CR1 (5-ring)
35	750	125.0	—
36	575	126.0	H, HC—5-ring
37	640	126.0	X (noH)—5-ring
38	770	126.0	OM—C—OM
39	760	132.0	5, 6 ring connection
40	2215	155.0	SI—OA—SI
41	91350	180.0	FE—C—O (CO bound to heme)
42	434	109.5	HWat—OWat—HWat
43	484	107.57	HChl—CChl—CLChl
44	632	111.30	CLChl—CChl—CLChl
45	469	97.4	CDmso—SDmso—CDmso
46	503	106.75	CDmso—SDmso—ODmso
47	443	108.53	HMet—OMet—CMet
48	618	109.5	CLCl4—CCl4—CLCl4
49	507	107.6	FTfe—CTfe—FTfe
50	448	109.5	HTfe—OTfe—CHTfe
51	524	110.3	OTfe—CHTfe—CTfe
52	532	111.4	CHTfe—CTfe—FTfe
53	636	117.2	NUrea—CUrea—NUrea
54	690	121.4	OUrea—CUrea—NUrea

Bond-angle types currently available in the 53A5 and 53A6 parameter sets. The atom names in the last column correspond to the atom types that are defined in Table 6. The seemingly large force constants for bond angle types 40 and 41 stem from the application of equation (10) for bond angles close to 180°. Parameters for (co)solvents (bond angle types 42—54) have often been parameterized to a higher accuracy, and are therefore presented here using a larger number of significant digits.

Table 4. Improper (harmonic) dihedral-angle parameters.

	Parameters for type I		
Improper dihedral-angle type code I	Force constant K_ξ (kJmol^{-1} degree^{-2})	Ideal improper dihedral angle ξ_0 (degree)	Example of usage
1	0.0510	0.0	planar groups
2	0.102	35.26439	tetrahedral centres
3	0.204	0.0	heme iron

Improper dihedral types currently available in the 53A5 and 53A6 parameter sets.

On the choice of the N_φ dihedral angles for a particular system the following guidelines can be given:

1. In general, for any bond between atoms j and k, only one set of atoms i, j, k, and l is chosen that define a dihedral angle.
2. For bonds between atoms j and k in rigid, planar rings (aromatics), no proper torsional dihedral angle is defined, but rather improper dihedrals are used to maintain the planarity of the ring.
3. To obtain correct torsional angle energy profiles, several torsional dihedral angles with different parameters can be defined on the same set of atoms i, j, k, and l. This is, for instance, done in sugar rings, or along the backbone of a nucleotide sequence.

In the GROMOS force field the parameters K_φ, δ, and m for torsional angles are defined over proper dihedral-angle types, which are together with the parameters values specified in Table 5. They have been selected such that the quantum-mechanical rotational energy profiles of torsional angles are reproduced by the proper torsional angle and third-neighbor or 1–4 nonbonded interaction terms of the GROMOS force field.

Nonbonded Interactions

In the GROMOS force field, nonbonded interactions are calculated over pairs of nonbonded atoms. In principle, all atom pairs should be included in this sum, but generally, the sum is restricted to a subset of atom pairs. First, covalently bound neighboring atoms (first neighbors) and second neighbors are standardly excluded from this sum. They are already directly interacting through the bonded interactions, and are thus considered to be excluded atom pairs for the nonbonded interactions. In addition, the third or 1–4 covalently bound neighbor atoms that are part of or bound to aromatic rings are also excluded from the nonbonded interactions. This makes it easier for the improper dihedral angle interactions to keep the atoms of and bound to a planar aromatic ring in one plane. Furthermore, there are a few exceptions to this general rule. These involve hydrogen atoms that have a repulsive van der Waals interaction equal to zero. In cases where the hydrogen is in a 1–4 or 1–5 covalently bound neighbor position to an oppositely charged atom, X45, and the heavy atom, X1, to which the hydrogen is bonded is an excluded atom with respect to atom X45 an additional exclusion of the hydrogen with atom X45 is sometimes needed. This is because the bonded interactions may fail to prevent the hydrogen atom from collapsing onto atom X45. For example, in the nucleotide adenosine atoms H61 and H62 are excluded from atom N7 for this reason.

Second, the sum over all pairs is restricted to those pairs that have an interatomic distance shorter than a specific cutoff distance. GROMOS distinguishes three ranges. The interactions that fall within a short cutoff length, R_p, are evaluated at every step in the simulation, usually from a pairlist that is constructed every N_p time steps. Each time the pairlist is constructed, the interactions between atoms separated by distances between R_p and a long range cutoff length R_l are also evaluated. These are then kept constant between pairlist updates. A reaction-field contribution from a homogeneous dielectric or ionic medium outside this large cutoff can finally be taken into account as a third, long-range electrostatic contribution (see below).

Van der Waals Interactions

The nonbonded van der Waals interactions are calculated as a sum over all interacting nonbonded atom pairs using a Lennard–Jones 12/6 interaction function with parameters C12 and C6,

$$V^{\mathrm{LJ}}(\mathbf{r}; s) = V^{\mathrm{LJ}}(\mathbf{r}; \mathrm{C12}, \mathrm{C6}) = \sum_{\text{pairs } i,j} \left(\frac{\mathrm{C12}_{ij}}{r_{ij}^{12}} - \frac{\mathrm{C6}_{ij}}{r_{ij}^{6}} \right). \quad (14)$$

The parameters $\mathrm{C12}_{ij}$ and $\mathrm{C6}_{ij}$ depend on the type of atoms involved and the character of the interaction. Table 6 describes the 53 different (nonbonded) atom types of the GROMOS force field. A united atom approach is chosen for aliphatic carbon groups, one "atom" represents both the carbon and the aliphatic hydrogens attached to it. The parameters $\mathrm{C12}_{ij}$ and $\mathrm{C6}_{ij}$ for atom pair i, j are obtained from $\mathrm{C12}_{ii}$, $\mathrm{C12}_{jj}$, and $\mathrm{C6}_{ii}$, $\mathrm{C6}_{jj}$ parameters, defined for each atom type, using the geometric combination rules[20]

$$\mathrm{C12}_{ij} = \sqrt{\mathrm{C12}_{ij} \cdot \mathrm{C12}_{jj}} \quad \mathrm{C6}_{ij} = \sqrt{\mathrm{C6}_{ii} \cdot \mathrm{C6}_{jj}}. \quad (15)$$

The choice of the parameters $\mathrm{C12}_{ii}$ and $\mathrm{C6}_{ii}$ to be used in (15) depends on the type of interaction the atoms i and j are involved in.

First, up to three different C12 parameters [C12(I), C12(II), and C12(III)] are defined for every atom. By default, C12(I) is used. However, polar and ionic interactions generally require a stronger van der Waals repulsion than interactions between neutral atoms. A slightly larger C12(II) is usually used if atoms i and j can form a hydrogen bond donor and acceptor pair to obtain the appropriate hydrogen bond length despite the favorable electrostatic interactions. To keep ionic groups with unlike charges at the appropriate distance, a slightly larger C12(III) is used for pairs that involve fully charged groups, such as ions. Table 7 lists the C6, C12(I), C12(II), and C12(III) parameters for different nonbonded atom types in the GROMOS force field. The choice of C12 parameter to be used for atom type I and atom type J in (15) is specified in the matrix shown in Table 8. We note that this matrix is not symmetric.

Second, in certain cases the GROMOS force field utilizes the possibility to use a different set of van der Waals interaction parameters if atoms i and j are connected via three covalent bonds.

Table 5. (Trigonometric) Torsional Dihedral-Angle Parameters.

	Parameters for type I			
Dihedral-angle type code I	Force constant K_φ (kJ/mol^{-1})	Phase shift cos(δ)	Multiplicity m	Examples of usage in terms of Nonbonded atom types
1	2.67	−1.0	1	CHn—CHn—CHn—OA (sugar) C4—C5—C6—O6[a]
2	3.41	−1.0	1	OA—CHn—OA—CHn, H (β sugar) O5—C1—O1—C1′, H1
3	4.97	−1.0	1	OA—CHn—CHn—OA (sugar) O5—C5—C6—O6[a]
4	5.86	−1.0	1	N—CHn—CHn—OA (lipid)
5	9.35	−1.0	1	OA—CHn—CHn—OA (sugar) O5—C5—C6—O6[b]
6	9.45	−1.0	1	OA—CHn—OA—CHn, H (α sugar) O5—C1—O1—C1′, H1
7	2.79	+1.0	1	P—O5*—C5*—C4* (dna)
8	5.35	+1.0	1	O5*—C5*—C4*—O4* (dna)
9	1.53	−1.0	2	C1—C2—CAB—CBB (heme)
10	5.86	−1.0	2	—C—C—
11	7.11	−1.0	2	—C—OA— (at ring)
12	16.7	−1.0	2	—C—OA—(carboxyl)
13	24.0	−1.0	2	CHn—OA—C—CHn (ester lipid)
14	33.5	−1.0	2	—C—N, NT, NE, NZ, NR—
15	41.8	−1.0	2	—C—CR1—(6-ring)
16	0.0	+1.0	2	—CH1 (sugar) —NR(base)—
17	0.418	+1.0	2	O—CH1—CHn—no O
18	2.09	+1.0	2	O—CH1—CHn—O
19	3.14	+1.0	2	—OA—P—
20	5.09	+1.0	2	CHn—O—P—O (dna, phosphodiester)
21	16.7	+1.0	2	—S—S—
22	1.05	+1.0	3	—OA—P—
23	1.26	+1.0	3	—CHn—OA— (no sugar)
24	1.30	+1.0	3	HTfe—OTfe—CHTfe—CTfe
25	2.53	+1.0	3	O5*—C5*—C4*—O4* (dna)
26	2.93	+1.0	3	—CH2—S—
27	3.19	+1.0	3	CHn—O—P—O (dna, phosphodiester)
28	3.65	+1.0	3	OA—CHn—OA—CHn, H (α sugar) O5—C1—O1—C1′, H1
29	3.77	+1.0	3	—C,CHn,SI—NT,NL,OA (sugar)—
30	3.90	+1.0	3	CHn—CHn—OA—H (sugar)
31	4.18	+1.0	3	HC—C—S—
32	4.69	+1.0	3	OA—CHn—OA—CHn, H (β sugar) O5—C1—O1—C1′, H1
33	5.44	+1.0	3	HC—C—C—
34	5.92	+1.0	3	—CHn,SI—CHn—
35	7.69	+1.0	3	OA—CHn—CHn—OA (sugar) O5—C5—C6—O6[a]
36	8.62	+1.0	3	N—CHn—CHn—OA (lipid)
37	9.50	+1.0	3	OA—CHn—CHn—OA (sugar) O5—C5—C6—O6[b]
38	0.0	+1.0	4	—NR—FE—
39	1.00	−1.0	6	—CHn—N,NE—
40	1.00	+1.0	6	—CHn—C,NR (ring), CR1—
41	3.77	+1.0	6	—CHn—NT—

Dihedral-angle types currently available in the 53A5 and 53A6 parameter sets. The atom names in the last column correspond to the atom types that are defined in Table 6.

[a]To be used if —C5—C6—O6 and adjacent —C4—O4— are one axial and the other equatorial, as in galactose.

[b]To be used if —C5—C6—O6 and adjacent —Cn—On—Hn are both simultaneously axial or equatorial, as in glucose.

Table 6. Nonbonded Atom Types and Integer Atom Codes.

Integer atom code	Atom type	Description
1	O	carbonyl oxygen (C═O)
2	OM	carboxyl oxygen (CO^-)
3	OA	hydroxyl or sugar oxygen
4	OE	ether or ester oxygen
5	OW	water oxygen
6	N	peptide nitrogen (NH)
7	NT	terminal nitrogen (NH2)
8	NL	terminal nitrogen (NH3)
9	NR	aromatic nitrogen
10	NZ	Arg NH (NH2)
11	NE	Arg NE (NH)
12	C	bare carbon
13	CH0	bare sp3 carbon, 4 bound heavy atoms
14	CH1	aliphatic or sugar CH-group
15	CH2	aliphatic or sugar CH2-group
16	CH3	aliphatic CH3-group
17	CH4	methane
18	CH2r	CH2-group in a ring
19	CR1	aromatic CH-group
20	HC	hydrogen bound to carbon
21	H	hydrogen not bound to carbon
22	DUM	dummy atom
23	S	sulfur
24	CU1+	copper (charge 1+)
25	CU2+	copper (charge 2+)
26	FE	iron (heme)
27	ZN2+	zinc (charge 2+)
28	MG2+	magnesium (charge 2+)
29	CA2+	calcium (charge 2+)
30	P, SI	phosphor or silicon
31	AR	argon
32	F	fluor (nonionic)
33	CL	chlorine (nonionic)
34	BR	bromine (nonionic)
35	CMet	CH3-group in methanol (solvent)
36	OMet	oxygen in methanol (solvent)
37	NA+	sodium (charge 1+)
38	CL−	chloride (charge 1−)
39	CChl	carbon in chloroform (solvent)
40	CLChl	chloride in chloroform (solvent)
41	HChl	hydrogen in chloroform (solvent)
42	SDmso	sulphur in DMSO (solvent)
43	CDmso	CH3-group in DMSO (solvent)
44	ODmso	oxygen in DMSO (solvent)
45	CCl4	carbon in carbontetrachloride (solvent)
46	CLCl4	chloride in carbontetrachloride (solvent)
47	FTfe	fluor in trifluoroethanol
48	CTfe	carbon in trifluoroethanol
49	CHTfe	CH2-group in trifluoroethanol
50	OTfe	oxygen in trifluoroethanol
51	CUrea	carbon in urea
52	OUrea	oxygen in urea
53	NUrea	nitrogen in urea

Atom types according to the integer atom code (IAC).

This separate definition of the so-called 1–4 interactions is needed to be able to simply reproduce torsional barriers of specific torsional angles. For the atom types for which special C6 and C12 parameters are defined in the case of 1–4 interactions, the corresponding van der Waals parameters are listed in Table 9.

Finally, there are cases where the combination rules of eq. (15) are not applied, and the interactions between specific atom types are directly defined through so-called mixed atom type pairs. Such cases are listed in Table 10.

Electrostatic Interactions

The electrostatic interactions between interacting pairs consist of three contributions. The first is a sum over all interacting pairs, using a Coulomb interaction V^{C}, with parameters q defined as the partial charges q_i on the atoms,

$$V^{\mathrm{C}}(\mathbf{r}; s) = V^{\mathrm{C}}(\mathbf{r}; q) = \sum_{\text{pairs } i,j} \frac{q_i q_j}{4\pi\varepsilon_0\varepsilon_1} \frac{1}{r_{ij}}, \tag{16}$$

where ε_0 is the dielectric permittivity of vacuum and ε_1 the relative permittivity of the medium in which the atoms are embedded. The value of ε_1 is standardly set to 1. In addition to the direct Coulombic interactions, a reaction-field contribution V^{RF} to the electrostatic interactions can be calculated, representing the interaction of atom i with the induced field of a continuous dielectric medium outside a cutoff distance, R_{rf}, due to the presence of atom j,[60]

$$V^{\mathrm{RF}}(\mathbf{r}; s) = V^{\mathrm{RF}}(\mathbf{r}; q) = \sum_{\text{pairs } i,j} \frac{q_i q_j}{4\pi\varepsilon_0\varepsilon_1} \frac{-\frac{1}{2} C_{rf} r_{ij}^2}{R_{rf}^3}, \tag{17}$$

where

$$C_{rf} = \frac{(2\varepsilon_1 - 2\varepsilon_2)(1 + \kappa R_{rf}) - \varepsilon_2(\kappa R_{rf})^2}{(\varepsilon_1 + 2\varepsilon_2)(1 + \kappa R_{rf}) + \varepsilon_2(\kappa R_{rf})^2} \tag{18}$$

and ε_2 and κ are the relative permittivity and inverse Debye screening length of the medium outside the cutoff sphere defined by R_{rf}, respectively. The sum in eq. (17) can also include the atom pairs that are excluded in the sum in eq. (16). Excluding the direct Coulomb interaction between atoms i and j should or need not change the electrostatic interaction between these atoms induced by the medium outside the cutoff. Hence, even though atom i might be excluded from atom j in eqs. (14) and (16), it should still feel the reaction field due to atom j, that is, should not be excluded from the sum in eq. (17).

Finally, the third term is sometimes referred to as a distance-independent reaction-field term. It is a constant (i.e., configuration independent) contribution to the energy for every pair that is taken into account,

$$V^{\mathrm{RFc}}(s) = V^{\mathrm{RFc}}(q) = \sum_{\text{pairs } i,j} \frac{q_i q_j}{4\pi\varepsilon_0\varepsilon_1} \frac{-(1 - \frac{1}{2} C_{rf})}{R_{rf}}. \tag{19}$$

As this term is independent of the interatomic distance r_{ij}, there is no contribution to the forces, but it ensures that the electrostatic energy is zero for atoms that are at the cutoff distance R_{rf}, thereby

Table 7. Normal van der Waals Parameters.

Integer atom code I	Atom type	$[C6(I,I)]^{1/2}$ $[(kJmol^{-1}\ nm^6)^{1/2}]$	$[C12(I,I)]^{1/2}$ $[10^{-3}(kJmol^{-1}\ nm^{12})^{1/2}]$		
			1	2	3
1	O	0.04756	1.000	1.130	—
2	OM	0.04756	0.8611	1.841	3.068
3	OA	0.04756	1.100	1.227	—
4	OE	0.04756	1.100	1.227	—
5	OW	0.05116	1.623	1.623	—
6	N	0.04936	1.523	1.943	—
7	NT	0.04936	1.523	2.250	—
8	NL	0.04936	1.523	3.068	—
9	NR	0.04936	1.523	1.841	—
10	NZ	0.04936	1.523	2.148	—
11	NE	0.04936	1.523	1.984	—
12	C	0.04838	2.222	—	—
13	CH0	0.04896	14.33	—	—
14	CH1	0.07790	9.850	—	—
15	CH2	0.08642	5.828	—	—
16	CH3	0.09805	5.162	—	—
17	CH4	0.1148	5.862	—	—
18	CH2r	0.08564	5.297	—	—
19	CR1	0.07425	3.888	—	—
20	HC	0.009200	0.1230	—	—
21	H	0.0	0.0	—	—
22	DUM	0.0	0.0	—	—
23	S	0.09992	3.616	—	—
24	CU1+	0.02045	0.07159	0.2250	—
25	CU2+	0.02045	0.07159	0.4091	—
26	FE	0.0	0.0	0.0	—
27	ZN2+	0.02045	0.09716	0.09716	—
28	MG2+	0.008080	0.05838	0.05838	—
29	CA2+	0.03170	0.7057	0.7057	—
30	P, SI	0.1214	4.711	4.711	—
31	AR	0.07915	3.138	—	—
32	F	0.03432	0.8722	1.227	—
33	CL	0.09362	3.911	—	—
34	BR	0.1663	8.092	—	—
35	CMet	0.09421	4.400	—	—
36	OMet	0.04756	1.525	1.525	—
37	NA+	0.008489	0.1450	0.1450	—
38	CL−	0.1175	10.34	10.34	10.34
39	CChl	0.051292	2.0160	—	—
40	CLChl	0.091141	3.7101	—	—
41	HChl	0.0061400	0.065574	—	—
42	SDmso	0.10277	4.6366	—	—
43	CDmso	0.098050	5.1620	—	—
44	ODmso	0.047652	0.86686	1.1250	—
45	CCl4	0.051292	2.7568	—	—
46	CLCl4	0.087201	3.5732	—	—
47	FTfe	0.034320	1.0000	1.0000	—
48	CTfe	0.048380	1.8370	—	—
49	CHTfe	0.084290	5.0770	—	—
50	OTfe	0.047560	1.2270	1.2270	—
51	CUrea	0.069906	3.6864	—	—
52	OUrea	0.048620	1.2609	1.2609	—
53	NUrea	0.057903	1.9877	1.9877	—

C6 and C12 parameters for the atom types.

Table 8. Selection of van der Waals (Repulsive) $[C12(I,I)]^{1/2}$ Parameters.

	J	1	2	3	4	5	6	7	8	9	10	11	24	25	26	27	28	29	30	32	33	34	36	37	38	44	47	50	52	53
I		O	OM	OA	OE	OW	N	NT	NL	NR	NZ	NE	CU1+	CU2+	FE	ZN2+	MG2+	CA2+	P, SI	F	CL	BR	OMet	NA+	CL−	ODmso	FTfe	OTfe	OUrea	NUrea
1	O	1	1	2	1	2	2	2	2	2	2	2	2	2	2	2	2	2	2	1	1	1	2	2	1	1	1	1	1	2
2	OM	1	1	2	1	2	2	2	3	2	3	3	3	3	3	3	3	3	3	1	1	1	2	3	1	1	1	1	1	2
3	OA	2	2	2	2	2	2	2	2	2	2	2	2	2	2	2	2	2	2	2	2	2	2	2	2	2	2	2	2	2
4	OE	1	1	2	1	2	2	2	2	2	2	2	2	2	2	2	2	2	2	1	1	1	2	2	1	1	1	1	1	2
5	OW	2	2	2	2	2	2	2	2	2	2	2	2	2	2	2	2	2	2	2	2	2	2	2	2	2	2	2	2	2
6	N	2	2	2	2	2	1	2	1	2	1	1	1	1	1	1	1	1	1	2	2	2	2	1	2	2	2	1	2	2
7	NT	2	2	2	2	2	2	2	2	2	2	2	1	1	1	1	1	1	1	2	2	2	2	1	2	2	2	2	2	2
8	NL	2	2	2	2	2	1	2	1	2	1	1	1	1	1	1	1	1	1	2	2	2	2	1	2	2	2	1	2	2
9	NR	2	2	2	2	2	2	2	2	2	2	2	2	2	2	2	2	2	2	2	2	2	2	2	2	2	2	2	2	2
10	NZ	2	2	2	2	2	1	2	1	2	1	1	1	1	1	1	1	1	1	2	2	2	2	1	2	2	2	1	2	2
11	NE	2	2	2	2	2	1	2	1	2	1	1	1	1	1	1	1	1	1	2	2	2	2	1	2	2	2	1	2	2
24	CU1+	2	2	2	2	2	1	1	1	2	1	1	1	1	1	1	1	1	1	2	2	2	2	1	2	2	2	1	2	1
25	CU2+	2	2	2	2	2	1	1	1	2	1	1	1	1	1	1	1	1	1	2	2	2	2	1	2	2	2	1	2	1
26	FE	2	2	2	2	2	1	1	1	2	1	1	1	1	1	1	1	1	1	2	2	2	2	1	2	2	2	1	2	1
27	ZN2+	2	2	2	2	2	1	1	1	2	1	1	1	1	1	1	1	1	1	2	2	2	2	1	2	2	2	1	2	1
28	MG2+	2	2	2	2	2	1	1	1	2	1	1	1	1	1	1	1	1	1	2	2	2	2	1	2	2	2	1	2	1
29	CA2+	2	2	2	2	2	1	1	1	2	1	1	1	1	1	1	1	1	1	2	2	2	2	1	2	2	2	1	2	1
30	P, SI	1	1	1	1	1	1	1	1	1	1	1	1	1	1	1	1	1	1	1	1	1	1	1	1	1	1	1	1	1
32	F	1	1	2	1	2	2	2	2	2	2	2	2	2	2	2	2	2	2	1	1	1	2	2	1	1	1	1	1	2
33	CL	1	1	1	1	1	1	1	1	1	1	1	1	1	1	1	1	1	1	1	1	1	1	1	1	1	1	1	1	1
34	BR	1	1	1	1	1	1	1	1	1	1	1	1	1	1	1	1	1	1	1	1	1	1	1	1	1	1	1	1	1
36	OMet	2	2	2	2	2	2	2	2	2	2	2	2	2	2	2	2	2	2	2	2	2	2	2	2	2	2	2	2	2
37	NA+	2	2	2	2	2	1	1	1	2	1	1	1	1	1	1	1	1	1	2	2	2	2	1	2	2	2	1	2	1
38	CL−	1	1	2	1	2	2	2	3	2	3	3	3	3	3	3	3	3	3	1	1	1	2	3	1	1	1	1	1	2
44	ODmso	1	1	2	1	2	2	2	2	2	2	2	2	2	2	2	2	2	2	1	1	1	2	2	1	1	1	2	1	2
47	FTfe	1	1	2	1	2	2	2	2	2	2	2	2	2	2	2	2	2	2	1	1	1	2	2	1	1	1	1	1	2
50	OTfe	1	1	2	1	2	1	2	1	2	1	1	1	1	1	1	1	1	1	1	1	1	2	1	1	2	1	2	2	2
52	OUrea	1	1	2	1	2	2	2	2	2	2	2	2	2	2	2	2	2	2	1	1	1	2	2	1	1	1	2	1	2
53	NUrea	2	2	2	2	2	2	2	2	2	2	2	1	1	1	1	1	1	1	2	2	2	2	1	2	2	2	2	2	2

For those atoms that have more than one C12 parameter defined in Table 7, this table defines which C12 parameter to use in the interaction with other atom types. For an atom pair with integer atom codes I and J, the $[C12(I,I)]^{1/2}$ value in formula (15) is taken from the fourth column in Table 7 if the matrix element (I,J) equals 1; it is taken from the fifth column if the matrix element is equal to 2, and from the sixth column if it is equal to 3. Similarly, the $[C12(J,J)]^{1/2}$ value in formula (15) is selected using the matrix element (J,I).

Table 9. Third-Neighbor or 1-4 van der Waals Parameters.

Integer atom code	Atom type	$[C6(I,I)]^{1/2}$ $[(kJmol^{-1}nm^6)^{1/2}]$	$(C12(I,I))^{1/2}$ $[10^{-3}(kJmol^{-1}nm^{12})^{1/2}]$		
			1	2	3
1	O	0.04756	0.8611	—	—
3	OA	0.04756	1.125	—	—
4	OE	0.04756	1.125	—	—
6	N	0.04936	1.301	—	—
7	NT	0.04936	1.301	—	—
8	NL	0.04936	1.301	—	—
9	NR	0.04936	1.301	—	—
10	NZ	0.04936	1.301	—	—
11	NE	0.04936	1.301	—	—
12	C	0.04838	1.837	—	—
13	CH0	0.04838	1.837	—	—
14	CH1	0.05396	1.933	—	—
15	CH2	0.06873	2.178	—	—
16	CH3	0.08278	2.456	—	—
18	CH2r	0.06873	2.178	—	—
19	CR1	0.07435	2.886	—	—

Van der Waals parameters to be used for atoms that are connected via three covalent bonds. If no value is specified, then the atom interacts via the normal van der Waals parameters defined in Table 7.

reducing cutoff noise in the energy. The sum in this term can also include the excluded pairs, as well as the self term i, i. This will make sure that the total contribution of the distance-independent reaction-field part is zero for neutral systems.

The charges that are used within the GROMOS force field are listed in Tables 11 to 15 for moieties or groups of atoms commonly found in biomolecular systems. In Table 11 two sets of charges are listed, one referred to as the 53A5 parameter set and one referred to as the 53A6 parameter set. The differences between these parameter sets will be explained in the following sections.

Parameterization

With the release of the GROMOS96 program[6] a new force field was also presented, in the form of the parameter set 43A1, which contained 43 individual atom types to describe biomolecular systems.[22] Shortly afterwards, some small changes in the torsional-angle parameters and the third-neighbor van der Waals interaction were introduced, to better reproduce the distribution of the torsional angle values in short aliphatic chains. This modification resulted in the 43A2 parameter set.[24] As it was then shown that the density for longer alkanes was too high, a reparameterization of the aliphatic united atoms followed, introducing two additional atom types for branched and cyclic alkanes, resulting in the 45A3 set of parameters.[9] The recent parameterization efforts regarding the description of sugars,[49] nucleotides,[53] and lipids[27] have resulted in the definition of a parameter set called 45A4. It involves a more accurate description of these molecules through the introduction and redefinition of several torsional angle parameters and through new charge distributions.

The reparameterization of aliphatic groups, resulting in the 45A3 parameter set[9] highlighted the need to also look closely at the parameters describing the polar groups in the GROMOS force field. This was especially apparent when it became evident that the free energy of hydration was consistently underestimated using the 43A2 parameter set in conjunction with the simple point charge (SPC)[42] model for liquid water.[50] In the current section we describe the derivation of the two new parameter sets, 53A5 and 53A6. Apart from a reparameterization of the polar groups, these parameter sets also include several recently parameterized (co-)solvents.[45,47,54,55] In parameter sets 53A5 and 53A6, many parameters have been redefined, and all interaction types have been renumbered with respect to the previous parameter sets to obtain a logical grouping of types.

Methods

The reparameterization of the polar groups in the GROMOS force field involved only the nonbonded interactions. No changes were made to the description of the bonded interactions with respect to previous parameter sets. The parameters were fitted based on two sets of data. First on the thermodynamic properties of the pure liquids of a series of 28 small molecules containing relevant functional groups listed in Table 16. Note, this set of compounds includes a relatively large number of esters. Esters form a crucial part of glycerides and lipids[25] but up till now little effort had been directed toward the parameterization of the ester group in the GROMOS force field. Second, on the free enthalpies of solvation in cyclohexane and in water of 14 representative compounds derived from the amino acids. These compounds consisted of the

Table 10. Normal van der Waals Parameters for Mixed Atom Type Pairs (I,J).

Integer atom code I	Atom type	Integer atom code J	Atom type	C6 (I,J) $10^{-3}kJmol^{-1}\ nm^6$	C12 (I,J) $10^{-6}kJmol^{-1}nm^{12}$
39	CChl	40	CLChl	4.6754	7.4813
39	CChl	41	HChl	0.3622	0.1745
40	CLChl	41	HChl	0.6493	0.3266

For the mixed atom type pairs, these parameters are used instead of the ones obtained through the combination rules in eq. (15).

Table 11. Atomic Charges for Amino-Acid Residues.

Atom name	53A5 Charge in *e*	53A6 Charge in *e*	Occurring in
N	−0.310	−0.310	all residues
H	0.310	0.310	
C	0.450	0.450	all residues
O	−0.450	−0.450	
CD	0.090	0.090	Arg (charge +1)
NE	−0.110	−0.110	
HE	0.240	0.240	
CZ	0.340	0.340	
NH1/2	−0.260	−0.260	
HH11/12/21/22	0.240	0.240	
NE	−0.310	−0.310	Argn (neutral)
HE	0.310	0.310	
CZ	0.208	0.266	Argn (neutral)
NH1	−0.611	−0.674	
HH1	0.403	0.408	
NH2	−0.830	−0.880	Argn (neutral)
HH21/22	0.415	0.440	
CG, CD	0.450	0.290	Asn, Gln
OD1, OE1	−0.450	−0.450	
ND2, NE2, NZ	−0.830	−0.720	Asn, Gln
HD21/22, HE21/22, HZ1/2	0.415	0.440	
CG, CD	0.270	0.270	Asp, Glu (charge −1)
OD1/2, OE1/2	−0.635	−0.635	
CG, CD	0.658	0.330	Asph, Gluh
OD1, OE1	−0.450	−0.450	
OD2, OE2	−0.611	−0.288	
HD2, HE2	0.403	0.408	
CB	−0.100	−0.100	Cys (charge −0.500)
SG	−0.400	−0.400	
CB	0.150	0.150	Cysh
SG	−0.350	−0.370	
HG	0.200	0.220	
CG	0.0	0.0	Hisa (proton at D1)
ND1	−0.310	−0.050	
HD1	0.310	0.310	
CD2	0.170	0.0	
HD2	0.100	0.140	
CE1	0.170	0.0	
HE1	0.100	0.140	
NE2	−0.540	−0.540	
CG	0.0	0.0	Hisb (proton at E2)
ND1	−0.540	−0.540	
CD2	0.170	0.0	
HD2	0.100	0.140	
CE1	0.170	0.0	
HE1	0.100	0.140	
NE2	−0.310	−0.050	
HE2	0.310	0.310	
CG	−0.050	−0.050	Hish (charge +1)
ND1	0.380	0.380	
HD1	0.300	0.300	
CD2	−0.100	−0.100	
HD2	0.100	0.100	
CE1	−0.340	−0.340	
HE1	0.100	0.100	
NE2	0.310	0.310	
HE2	0.300	0.300	
CG, CB, CB	0.208	0.266	Hyp, Ser, Thr
OD1, OG, OG1	−0.611	−0.674	
HD1, HG, HG1	0.403	0.408	
CE	0.127	0.127	Lysh (charge +1)
NZ	0.129	0.129	
HZ1/2/3	0.248	0.248	
CE	0.0	−0.240	Lys (neutral)
NZ	−0.830	−0.640	
HZ1/2	0.415	0.440	
CG, CE	0.150	0.241	Met
SD	−0.300	−0.482	
CG	0.0	−0.210	Trp
CD1	−0.146	−0.140	
HD1	0.146	0.140	
CD2	0.0	0.0	
NE1	−0.310	−0.100	
HE1	0.310	0.310	
CE2	0.0	0.0	
CZ	0.208	0.203	Tyr
OH	−0.611	−0.611	
HH	0.403	0.408	
C	−0.146	−0.140	all aromatic C—H groups in Phe, Tyr, Trp
H	0.146	0.140	
C	−0.292	0.0	aromatic C connected to an aliphatic CHn in Phe, Tyr
CH2	0.292	0.0	aliphatic CHn connected to aromatic C in Phe, Tyr

For every residue the charges of nonneutral atoms are given in the second (53A5) and the third (53A6) column. Atoms that are not listed have a zero charge. Functional groups of small compounds in the current parameterization that were not directly derived from amino acid residues were defined by analogy.

Table 12. Atomic Charges for Various (Co)solvents.

Atom name	Charge in *e*	Occurring in
OW	−0.82000	H_2O (SPC model)[a]
HW1/2	0.41000	
OW	−0.84760	H_2O (SPC/E model)[b]
HW1/2	0.42380	
OW	−0.68850	H_2O (SPC/L model)[c]
HW1/2	0.34425	
CChl	0.17900	Chloroform[d]
CLChl	−0.08700	
HChl	0.08200	
SDmso	0.12753	DMSO[e]
CDmso	0.16000	
ODmso	−0.44753	
CMet	0.26600	Methanol[f]
OMet	−0.67400	
HMet	0.40800	
CCl4	0.0	Carbontetrachloride[g]
CLCl4	0.0	
FTfe	−0.17000	2,2,2-Trifluoroethanol[h]
CTfe	0.45200	
CHTfe	0.27300	
OTfe	−0.62500	
HTfe	0.41000	
CUrea	0.14200	Urea[i]
OUrea	−0.39000	
NUrea	−0.54200	
HUrea	0.33300	

Solvent charges for 53A5 and 53A6 parameter sets. See [a]ref. 42; [b]ref. 92; [c]ref. 43; [d]ref. 44; [e]ref. 47; [f]ref. 45; [g]ref. 48; [h]ref. 54; [i]ref. 55.

Table 14. Atomic Charges for Lipids.

Atom name	Charge in *e*	Occurring in
C32, C33, C34, C35	0.250	dppc
N	0.0	dppc
C31	0.0	dppc
O31, O32	−0.360	dppc
O33, O34	−0.635	dppc
P	0.990	dppc
C3	0.0	dppc
C1, C2	0.160	dppc
O11, O21	−0.360	dppc
O12, O22	−0.380	dppc
C11, C21	0.580	dppc
C12, . . . , C22, . . .	0.0	dppc

Lipid charges are the same for both parameter sets.

neutral forms of the amino acid side chains, where the CB atom CH_n has been replaced by CH_{n+1}. Note, for the histidine analog (methyl imidazole) the aromatic hydrogens bonded to carbon atoms were included explicitly to be consistent with other aromatic groups. A similar adaptation has been applied to the nucleotide bases in the 45A4 parameter set. We focused on the neutral forms of the amino acid analogs to be able to directly compare with experimental solvation free enthalpies.[61,62] Of course, when simulating a biomolecular system at physiological pH, the side chains of arginine, aspartic acid, glutamic acid, and lysine will, in most cases, be charged. The parameterization of these charged states will be the subject of a subsequent study.

Table 13. Atomic Charges for Nucleotides.

Atom name	Charge in *e*	Occurring in
O3/5*	−0.360	all nucleotides
P	0.990	
O1/2P	−0.635	
C4*	0.160	all nucleotides
O4*	−0.360	
C1*	0.200	
N9, N9, N1, N1, N1	−0.200	dAde, dGua, dCyt, dThy, Ura
C4, C4	0.200	dAde, dGua
C6, C6, C6	0.100	dCyt, dThy, Ura
H6, H6, H6	0.100	dCyt, dThy, Ura
N1, N3, N7, N3, N7, N3	−0.540	dAde, dAde, dAde, dGua, dGua, dCyt
C2, C8, C8	0.440	dAde, dAde, dGua
H2, H8, H8	0.100	dAde, dAde, dGua
C6, C2, C4	0.540	dAde, dGua, dCyt
N6, N2, N4	−0.830	dAde, dGua, dCyt
H61/62, H21/22, H41/42	0.415	dAde, dGua, dCyt
N1, N3, N3	−0.310	dGua, dThy, Ura
H1, H3, H3	0.310	dGua, dThy, Ura
C6, C2, C2, C4, C2, C4	0.450	dGua, dCyt, dThy, dThy, Ura, Ura
O6, O2, O2, O4, O2, O4	−0.450	dGua, dCyt, dThy, dThy, Ura, Ura
C5, C5	−0.100	dCyt, Ura
H5, H5	0.100	dCyt, Ura

Nucleotide charges are the same for both parameter sets. Atoms that are not listed have a zero charge.

Table 15. Atomic Charges for Carbohydrates.

Atom name	Charge in *e*	Occurring in
C1, C2, C3, C6	0.232	glucopyranose, polyuronate, terminal—CHn—On—Hn group
O2, O3, O6	−0.642	glucopyranose, polyuronate, terminal—CHn—On—Hn group
HO2, HO3, HO6	0.410	glucopyranose, polyuronate, terminal—CHn—On—Hn group
C5	0.376	glucopyranose, polyuronate
O5	−0.480	glucopyranose, polyuronate
O1	−0.360	glucopyranose, polyuronate
C4	0.232	glucopyranose, polyuronate
C6	0.360	polyuronate
O61, O62	−0.680	polyuronate
C1	0.232	terminal—C1—O1—CM group
O1	−0.360	terminal—C1—O1—CM group
CM (methyl)	0.232	terminal—C1—O1—CM group

Carbohydrate charges are the same for both parameter sets.

The pure liquid simulations were carried out using the GROMOS96 simulation package.[6,56] Initial coordinates were generated by arranging 343 or 512 molecules on a cubic periodic grid corresponding to the experimental density. After a steepest descent minimization to remove bad contacts between molecules, initial velocities were assigned from a Maxwell–Boltzmann distribution, corresponding to a temperature of 298 K (or at the boiling point of the liquid at normal pressure, if this was lower). The system was first equilibrated for about 100 ps at constant volume, after which another 100 ps of equilibration at constant pressure was carried out. Finally, the systems were simulated for 400 ps from which the average density and heat of vaporization were calculated. All bond lengths were constrained, using the SHAKE algorithm[63] with a relative geometric accuracy of 10^{-4}, allowing for a time step of 2 fs. The temperature (298 K or at the boiling point if this was lower) and pressure (1 atm) were kept constant using the weak coupling approach,[64] with $\tau_T = 0.1$ ps and $\tau_P = 0.5$ ps to correspond to the thermodynamic state point at which many biomolecular simulations are performed. The isothermal compressibilities were either taken directly from experiment or estimated from the difference in pressure between two short (10 ps) constant volume

Table 16. Densities and Heats of Vaporization for Pure Liquids.

	45A3		53A5		Experiment	
Compound	ρ (kg m^{-3})	ΔH^{vap} (kJ mol^{-1})	ρ (kg m^{-3})	ΔH^{vap} (kJ mol^{-1})	ρ (kg m^{-3})	ΔH^{vap} (kJ mol^{-1})
Methanol	781	36.1	787	37.4	784[a]	37.4[a]
Ethanol	763	39.8	778	44.3	785[a]	42.3[a]
2-Propanol	730	37.8	740	42.3	885[a]	45.5[a]
1-Butanol	708	48.0	774	52.4	806[a]	52.3[a]
Diethylether	731	27.4	722	27.0	708[a]	27.2[a]
Acetone	678	31.7	653	31.3	784[a]	31.3[a]
2-Butanone	834	33.5	826	34.5	800[a]	34.5[a]
3-Pentanone	821	36.2	805	36.0	809[a]	38.5[a]
Acetic acid	1184	47.4	1147	48.5	1044[a]	51.6[b]
Methyl acetate	1017	36.1	977	33.2	928[a]	32.3[a]
Ethyl acetate	960	37.6	927	34.6	895[a]	35.6[c]
Ethyl propanoate	923	40.3	899	37.8	884[a]	39.3[c]
Ethyl butanoate	909	45.1	890	42.9	874[a]	42.7[c]
Propyl acetate	933	41.3	908	38.6	883[a]	39.8[a]
Butyl acetate	920	46.0	897	43.2	876[a]	43.6[a]
Ethyl glycol dipropanoate	1073	72.5	1042	71.5	1036[c]	67.6[c]
Glycerol tripropanoate	1108	99.2	1078	92.2	1076[c]	91.4[c]
Ethane amine	798	47.4	725	29.3	683[d]	28.7[d]
1-Butane amine	797	49.6	745	30.1	737[a]	35.7[a]
1,2-Ethane diamine	1028	83.5	979	51.1	893[a]	46.7[a]
Diethyl amine	717	31.5	716	31.1	702[a]	31.3[b]
N-Methyl acetamide	989	47.9	964	51.6	950[a]	59.4[a]
Benzene	982	37.7	901	32.5	874[a]	33.8[a]
Toluene	937	36.2	901	37.2	862[a]	38.0[a]
Dimethylsulfide	852	25.8	850	25.7	842[e]	27.7[f]
Ethanethiol	917	28.3	919	28.4	833[g]	27.5[f]
Ethylmethylsulfide	842	29.8	840	29.6	837[g]	31.8[h]
Dimethyldisulfide	1118	37.4	1118	37.4	1057[g]	38.4[f]

Comparison of calculated values using parameter sets 45A3 and 53A5 to experimental ones. Experimental values are from [a]ref. 74; [b]ref. 75; [c]ref. 76; [d]ref. 77; [e]ref. 79; [f]ref. 81; [g]ref. 78; [h]ref. 80.

simulations in which the density was increased and decreased by 5% with respect to the experimental value. Nonbonded interactions were calculated using a triple range scheme. Interactions within a short range cutoff of 0.8 nm were calculated every time step from a pairlist that was generated every five steps. At these time points, interactions between 0.8 and 1.4 nm were also calculated and kept constant between updates. A reaction-field contribution[60] was added to the electrostatic interactions and forces to account for a homogeneous medium outside the long-range cutoff, using the experimental value for the relative permittivity of the liquid. The reaction-field contributions (17) and (19) were included for atoms that were excluded from the direct Coulombic interaction (16) as was the self-term.

Additional simulations were carried out for gaseous systems in which the individual molecules were separated by at least 50 nm, effectively corresponding to a vacuum simulation. All remaining simulation settings were unchanged except for the reaction-field contributions to the long-range electrostatic interactions that were not calculated. The heat of vaporization ΔH_{vap} of the liquids were calculated from the potential energies in the gaseous (U_{pot}^{gas}) and liquid phases (U_{pot}^{liq}) as

$$\Delta H_{vap} = \Delta U_{vap} + p\Delta V_{vap} = U_{pot}^{gas} - U_{pot}^{liq} + RT, \qquad (20)$$

where p is the pressure, T is the temperature, and R is the gas constant.

The free enthalpies of solvation were calculated using the GROMACS[65–67] (cyclohexane) and the GROMOS[6,56] (water) simulation packages. The SPC model[42] was used for water. All solute molecules were solvated in truncated octahedral boxes filled with equilibrated solvent molecules. Box sizes were chosen such that no solvent molecule interacted with more than one periodic image of the solute. Simulation conditions were the same as described above, with isothermal compressibilities of $11.2 \cdot 10^{-4}$ (cyclohexane; coupling time $\tau_P = 2.0$ ps) and $4.575 \cdot 10^{-4}$ [(kJ mol^{-1} nm^{-3})$^{-1}$] (water; coupling time $\tau_P = 0.5$ ps). The relative permittivity for the reaction field was set to 6 for cyclohexane and to 62 for SPC.[68]

The free enthalpy of solvation was calculated using the thermodynamic integration (TI) approach.[69] To remove the solute from the system all nonbonded interactions involving solute atoms were scaled down to zero in a stepwise manner as a function of a coupling parameter λ. The free enthalpy change corresponding to the removal of all solute nonbonded interactions was then calculated by integrating the average value of the derivative of the total Hamiltonian of the system with respect to λ,

$$\Delta G = \int_0^1 \left\langle \frac{\partial H}{\partial \lambda} \right\rangle_\lambda d\lambda. \qquad (21)$$

The integral above was evaluated using 21 evenly spaced λ-points with 50 ps of equilibration and 150 ps of data collection at each point. A soft-core interaction was used to avoid singularities in the nonbonded interaction function at intermediate λ-values.[70] The free enthalpy of solvation was calculated as the difference between the free enthalpy change calculated from a vacuum simulation of the solute and the free enthalpy change when the solute is in solution.

In general, when deriving the new parameter sets, the attractive C6 van der Waals parameters were not changed, as these have an experimental origin being obtained from atomic polarizabilities.[1,2,20,58] The parameterization efforts were focused on the repulsive term C12 and on the atomic charges of the polar groups. In an iterative procedure, the nonbonded parameters of the polar groups were modified to reproduce the densities and heats of vaporization considering the whole range of pure liquids. The aim was to obtain a limited and consistent set of parameters with the same (or similar) parameters being used to describe similar atoms in different functional groups and molecules. For this reason, the iteration of the parameters was performed manually. A manual procedure was preferred over an automated procedure[71–73] because chemical intuition was needed to balance the results for different groups, and to ensure that the final values reflected the relative importance of different functional groups in biomolecular systems. The parameters obtained were then used to calculate free enthalpies of solvation in water and cyclohexane. This cycle was repeated until a parameter set was obtained that was able to reproduce the densities and heats of vaporization of the pure liquids as well as the free enthalpy of solvation in cyclohexane with reasonable accuracy. Reproducing the free enthalpies of hydration was more problematic. Despite many attempts at optimization it proven not possible to simultaneously reproduce the properties of the pure liquids, the free enthalpies of solvation in cyclohexane, and the free enthalpies of hydration. To reproduce the experimental free enthalpies of hydration a different set of charges that could not be used in the pure liquids were needed. The consequences of this will be discussed in detail in the following sections.

Results and Discussion

Tables 16 to 18 and Figures 1 to 4 show the densities, heats of vaporization, and free enthalpies of solvation for the different parameter sets together with the corresponding experimental values for all compounds studied. The force fields considered here are the original GROMOS 43A2 and 45A3 force fields, which were the starting points of the parameterization, and the 53A5 and 53A6 force fields that are the result of the reparameterization reported here. The parameters for the 53A5 and 53A6 force fields are listed in Tables 1 to 15. Experimental data were taken from the literature at temperatures corresponding to the simulation temperatures.[61,62,74–81]

Figures 1–4, which display graphically the values represented in Tables 16 and 17 clearly show that the 53A5 parameter set is an improvement over the 45A3 parameter set in terms of the density and heat of vaporization of the pure liquids and the free enthalpy of solvation in cyclohexane. For the 28 compounds investigated as liquids, the average deviation from the experimental density decreases from 7% (45A3) to less than 4% (53A5), while the average absolute deviation in the heat of vaporization is reduced from 5.1 kJ/mol (45A3) to 1.8 kJ/mol (53A5). This indicates that the description of the interactions of specific polar groups with themselves has been improved. In most cases, reparameterization in-

Table 17. Free Enthalpies of Solvation in Cyclohexane for Amino-Acid Analogs.

Amino-acid analog	43A2[a]	45A3	53A5/53A6	Experiment
Arg	−24.0	−24.3	−18.6	−20.6
Asn	−14.3	−15.3	−12.8	−12.6
Asp	−15.6	−15.5	−15.1	−9.2
Cys	−7.9	−8.7	−8.7	−10.3
Gln	−19.3	−18.2	−14.8	−13.9
Glu	−18.6	−18.7	−18.4	−15.8
His	−21.1	−23.0	−19.6	−23.4
Lys	−16.8	−14.0	−11.2	−16.4
Met	−14.4	−16.9	−17.2	−15.8
Phe	−25.2	−24.6	−19.9	−19.6
Ser	−3.5	−4.5	−5.3	−6.9
Thr	−7.8	−7.9	−8.3	−9.5
Trp	−35.9	−37.0	−29.8	−33.4
Tyr	−28.3	−27.1	−25.2	−24.6

Comparison of calculated values using parameter sets 43A2, 45A3, and 53A5 to experimental ones.
[a]Taken from ref. 50. Experimental values were taken from ref. 61. The analogs of Arg, Asp, Glu, and Cys were modeled in their neutral form.

volved increasing both the C12 interaction parameters and the partial charges (dipoles). The absolute mean deviation in the free enthalpy of solvation in cyclohexane improved from 3.1 kJ/mol (43A2) and 2.9 kJ/mol (45A3) to 2.2 kJ/mol (53A5). Because no charges are involved in the interaction with cyclohexane, the improvement in the free enthalpy of solvation in this medium indicates that the parameters used to describe the van der Waals interactions in the liquids perform well in combination with the (recently developed) aliphatic van der Waals parameters.[9] All have now been parameterized with a cutoff of 1.4 nm. In water, how-

Table 18. Free Enthalpies of Solvation in Water for Amino-Acid Analogs.

Amino-acid analog	43A2	45A3	53A5	53A6	Experiment
Arg	−36.4	−35.5	−40.4	−46.1	−45.7
Asn	−18.9	−19.7	−25.0	−40.6	−40.6
Asp	−14.9	−16.3	−16.8	−30.6	−28.0
Cys	5.1	3.2	−4.1	−4.7	−5.2
Gln	−17.8	−16.6	−21.0	−38.5	−39.4
Glu	−16.2	−13.5	−13.5	−27.2	−27.0
His	−27.9	−27.9	−26.7	−42.7	−42.9
Lys	−7.5	−5.4	−3.7	−17.3	−18.3
Met	7.0	7.0	3.3	−6.8	−6.2
Phe	−2.0	−2.6	−12.2	0.0	−3.1
Ser	−14.2	−15.1	−16.9	−22.1	−21.2
Thr	−12.4	−13.0	−15.3	−20.0	−20.5
Trp	−13.5	−12.1	−14.6	−25.7	−24.7
Tyr	−25.0	−25.5	−36.7	−25.5	−26.6

Comparison of calculated values using parameter sets 43A2, 45A3, 53A5, and 53A6 to experimental ones. Experimental values were taken from ref. 62. The analogs of Arg, Asp, Glu, and Cys were modeled in their neutral form.

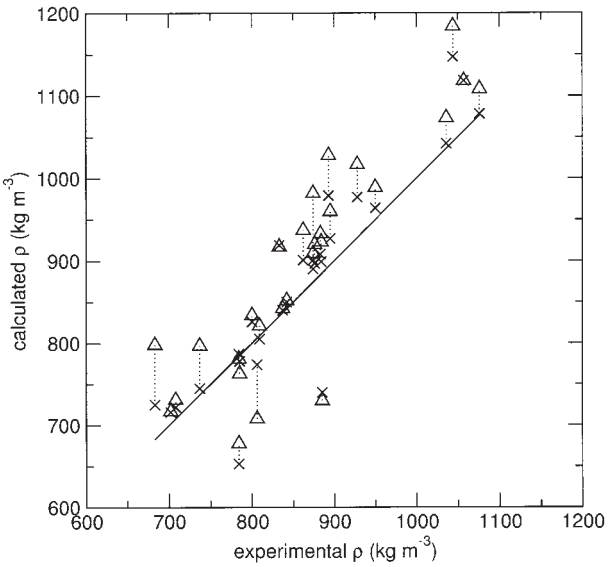

Figure 1. Density for pure liquids. Comparison of experimental densities to calculated values obtained using parameter sets 45A3 (triangles) and 53A5 (crosses) for the 28 compounds listed in Table 16. Diagonal line corresponds to perfect agreement with experiment. Dotted lines are drawn to facilitate comparison between values for the same compound obtained with different parameter sets.

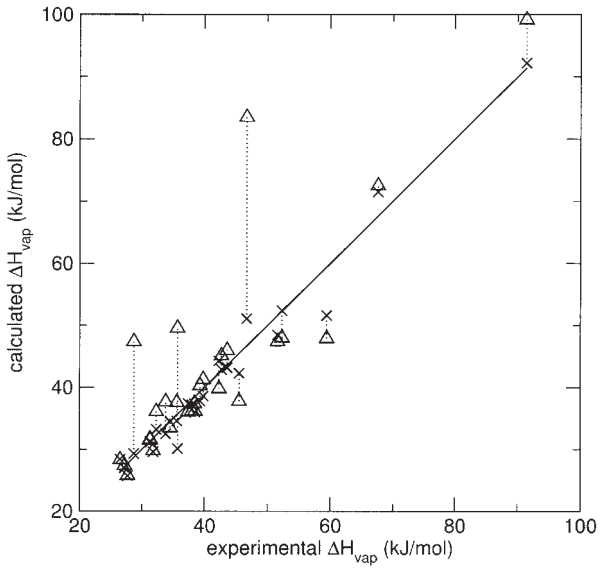

Figure 2. Heat of vaporization for pure liquids. Comparison of experimental heats of vaporization to calculated values obtained using parameter sets 45A3 (triangles) and 53A5 (crosses) for the 28 compounds listed in Table 16. Diagonal line corresponds to perfect agreement with experiment. Dotted lines are drawn to facilitate comparison between values for the same compound obtained with different parameter sets.

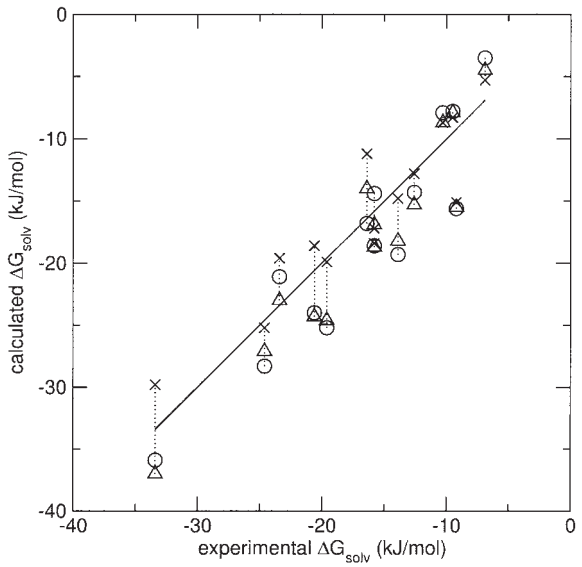

Figure 3. Free enthalpies of solvation in cyclohexane. Comparison of experimental free enthalpies of solvation to calculated values obtained using parameter sets 43A2 (circles), 45A3 (triangles), and 53A5 (crosses) for the 14 compounds listed in Table 17. Diagonal line corresponds to perfect agreement with experiment. Dotted lines are drawn to facilitate comparison between values for the same compound obtained with different parameter sets.

ever, the 53A5 parameter set does not represent a significant improvement over the original 45A3 parameter set in terms of the hydration free enthalpies of the compounds investigated (see Fig. 4). The average absolute error calculated from Table 18 decreased only slightly from 11.2 kJ/mol (45A3) to 10.3 kJ/mol (53A5).

The free enthalpy of hydration is primarily dependent on the partial charges on the solutes. It is relatively insensitive to the van der Waals parameters. To reproduce the free enthalpies of hydration larger partial charges (dipoles) within the solutes are required. The properties of the pure liquids, however, are highly sensitive to the balance between the van der Waals parameters and partial charges. For almost all functional groups we could not find a combination of a charge distribution and a set of van der Waals parameters that would reproduce the free enthalpy of hydration while simultaneously reproducing the density and heat of vaporization of the pure liquid. That is, without using van der Waals parameters that would be incompatible with the rest of the force field. For example, using the 53A6 charges to simulate pure liquid methanol, ethanol, ethane amine, or 1-butane amine results in a deviation from experiment of about 10% in the density and 8 kJ/mol in the heat of vaporization. For benzene, the deviations are smaller (3% and 4 kJ/mol, respectively). The ether and ketones, on the other hand, have the same charges in both parameter sets and thus yield the same density and heat of vaporization.

That it is impossible to obtain a single set of partial charges that are appropriate in all environments is not surprising. The overall charge distribution within a molecule is determined by the relative electronegativities of individual atoms together with polarization effects induced by the environment. In nonpolarizable force fields such as GROMOS, AMBER, CHARMM, and OPLS the charge distribution is statically assigned. The average effect of polarization in a given environment is incorporated implicitly into the model by a specific combination of van der Waals parameters and partial charges. For example, the partial charges of the SPC water model result in a molecular dipole of 2.27 D. This is much larger than the experimental gas phase dipole (1.85 D), but allows for a very accurate reproduction of a wide range of bulk water properties.[42,43,82] The charges that were derived from the pure liquids in the 53A5 parameter set reflect the average polarization in the liquid phase of the compound. It is clear that for most compounds the degree of polarization will be greater when the isolated compound is solvated in water. Thus, enhanced partial charges are required to obtain the correct free enthalpy of hydration.

The only true solution to this problem would be the explicit treatment of polarization within the model. This has, however, a high computational overhead and would require the complete reparameterization of the force field. Here we present an intermediate approach. The 53A5 parameter set is a consistent set of parameters that reproduces the thermodynamic properties of a range of pure liquids and the solvation enthalpies of a set of amino acid analogues in nonpolar or weakly polar environments. The 53A6 parameter set, in contrast, has been specifically adjusted to reproduce the free enthalpies of hydration in SPC water. Note, only the charges have been adjusted; the bonded and van der Waals interactions used in the 53A6 parameter set are identical to the 53A5 parameter set. This means that the free enthalpy of solvation in cyclohexane is almost unchanged when using the 53A6 parameter set as only intermolecular electrostatic terms are

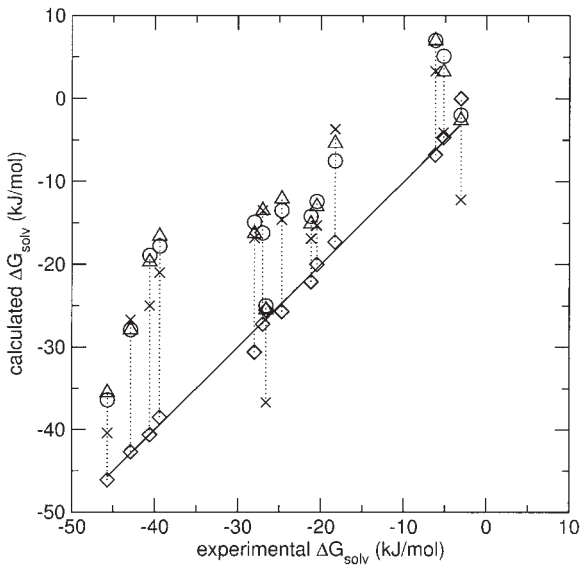

Figure 4. Free enthalpies of solvation in water. Comparison of experimental free enthalpies of solvation to calculated values obtained using parameter sets 43A2 (circles), 45A3 (triangles), 53A5 (crosses), and 53A6 (diamonds) for the 14 compounds listed in Table 18. Diagonal line corresponds to perfect agreement with experiment. Dotted lines are drawn to facilitate comparison between values for the same compound obtained with different parameter sets.

affected. The 53A6 parameter set reproduces the free enthalpy of hydration in SPC water for the set of amino acid analogs studied with an average absolute error of only 0.9 kJ/mol and also correctly reproduces the partitioning behavior of these analogs between water and a hydrophobic environment.

The GROMOS force field has been primarily developed as a tool for simulating biomolecular systems. The question thus is: which set of charges is most appropriate to simulate a biomolecular system? In protein folding simulations, for example, a specific polar group may interact both with the strongly polarizable solvent (water), and with the (probably) less polarizable environment within the protein. To address this question we consider two factors. First, most biomolecular systems simulated consist largely of water, and thus overall the system more closely resembles an aqueous phase. Second, polar groups in proteins, DNA, and lipids are predominantly located close to water molecules of the solvent, leading to a larger number of interactions of the polar groups with water molecules than with themselves. For these reasons we suggest that the use of the 53A6 force field is most appropriate for simulating complex heterogeneous systems involving water as a solvent. Both the 53A5 and 53A6 parameter sets show good agreement with the free enthalpies of solvation in cyclohexane. This indicates that the van der Waals interaction with aliphatic groups is described well. The interaction of the aliphatic groups with water has been shown previously to correspond well to the experiment.[9] Correspondingly, in the 53A6 parameter set the polar groups have a correct interaction with water, whereas in the 53A5 parameter set only the self-interaction between polar groups in the pure liquid phase is optimized. As far as the interaction between different polar groups is concerned, neither of the parameter sets has been parameterized specifically on these interactions. In the 53A6 parameter set, however, the polar groups all have two mutual interaction partners (water and cyclohexane) that seem to be represented reasonably well. In an aqueous medium, this puts most trust in the interaction between polar groups. The current parameters must, nevertheless, still be validated[41] by extensive use in practical biomolecular applications. This work is currently being carried out. Three other well-known force fields, AMBER, CHARMM, and OPLS-AA have been tested recently in simulations of three proteins, leading to the conclusion that these force fields behave comparably in simulations[83] or at least that it was not possible to distinguish between the force fields on the 2-ns time scale investigated.

To our knowledge, no other biomolecular force field has been specifically parameterized to reproduce free enthalpies of solvation. Solvation free enthalpies and similar properties have, however, been previously calculated for the same set of compounds considered here using different force fields, water models, and methods.[50–52,84–87] Shirts et al.,[51] in particular, compared the free enthalpies of hydration for 15 compounds (including four aliphatic compounds) using the AMBER(ff94), CHARMM22, and OPLS-AA force fields together with the TIP3P water model. Using much computational power, they obtained extremely precise values with average absolute errors when compared to experiment of 5.1 kJ/mol (AMBER), 4.4 kJ/mol (CHARMM), and 3.1 kJ/mol (OPLS-AA). Using the current 53A6 parameters, we obtained (see Table 18) an average absolute error of 0.9 kJ/mol for 14 polar compounds. Including the results for aliphatic compounds published previously,[9] we obtain an average error of 0.8 kJ/mol for the same 15 compounds investigated by Shirts et al. The corresponding values for the 43A2 parameter set are 11.1 kJ/mol and 8.7 kJ/mol, for the 45A3 parameter set 11.2 kJ/mol and 8.4 kJ/mol, and for the 53A5 parameter set 10.3 kJ/mol and 7.9 kJ/mol.

Recently, the free energy surface of the peptide backbone as function of the ϕ- and ψ-torsional angles has also been compared for several biomolecular force fields.[88–90] Based on the fact that the force fields produce different ϕ-/ψ-probability distributions, Hu et al.[89] concluded that none of the current force fields are accurate enough to describe the conformations of an unfolded polypeptide. The results of Mu et al.,[90] however, suggest that the description of the ϕ-/ψ-distribution by the GROMOS force field (set 45A3) is reasonable. We note in this regard that the third-neighbor van der Waals interaction parameters (Table 9) are unchanged between the 45A3 and 53A5/53A6 GROMOS parameter sets. Thus, the conclusions of the studies mentioned above concerning the free energy surface of the peptide backbone are likely to still be approximately valid for the current parameter sets.

Conclusions

The two most recent parameter sets of the GROMOS force field, 53A5 and 53A6, have been described and discussed. These parameters are the result of an extensive reparameterization of a number of polar (noncharged) groups as well as the inclusion of previously parameterized (co)solvents. With respect to the previous parameter sets (45A3 and 45A4), all atom, bond, bond-angle, improper dihedral-angle, and torsional dihedral-angle types have been renumbered and several new types have been added.

Within the degrees of freedom that we allowed ourselves for the parameterization, it was not possible to obtain a set of charges for the polar groups investigated that could simultaneously reproduce the thermodynamic properties of a range of pure liquids and the solvation enthalpy of hydration with high accuracy. The most likely physical explanation for this is that the differences in polarization of the solute in the two phases cannot adequately be represented using a single charge distribution. Polarization is not explicitly included in either the GROMOS force field or any of the other force fields commonly used for simulating biomolecular systems. It is becoming clear, however, that we are reaching the limit of purely classical nonpolarizable force fields. For this reason, we have presented two alternative parameter sets that have been tuned for different phases. The development of a fully polarizable version of the GROMOS force field is underway.[91]

Because the free enthalpy of hydration is a key thermodynamic property in many biomolecular processes of interest, we recommend the use of the 53A6 parameter set for simulations of biomolecules in explicit water. This parameter set shows good agreement with solvation free enthalpies in both cyclohexane and water. It is important that these new parameter sets be further validated in simulations of biomolecular systems containing proteins, DNA, sugars, and lipids. However, as these parameter sets have improved hydration and solvation properties, one would expect improved results in polypeptide folding simulations and in the prediction of interaction constants between biomolecules in the aqueous phase.

Acknowledgments

The authors would like to acknowledge the fact that many persons contributed to the development of the GROMOS force field over the past decades. In particular: Indira Chandrasekhar for the lipid parameters, Roberto Lins for the sugar parameters, and Thereza Soares for the nucleotide parameters. Furthermore, we would like to thank Robert Woody for supplying the latest heme parameters, Ulf Börjesson for pointing out inconsistencies in the amine parameters, and Alex de Vries for useful discussions on the proper treatment of reaction-field electrostatics.

References

1. Hünenberger, P. H.; van Gunsteren, W. F. In Computer Simulation of Biomolecular Systems, Theoretical and Experimental Applications; van Gunsteren, W. F.; Weiner, P. K.; Wilkinson, A. J., Eds.; Kluwer Academic Publishers: Dordrecht, 1997, p. 3.
2. Hünenberger, P. H.; van Gunsteren, W. F. In Potential Energy Surfaces; Sax, A. F., Ed.; Springer: Berlin, 1999, p. 177.
3. Cornell, W. D.; Cieplak, P.; Bayly, C. I.; Gould, I. R.; Merz, K. M.; Ferguson, D. M.; Spellmeyer, D. C.; Fox, T.; Caldwell, J. W.; Kollman, P. A. J Am Chem Soc 1995, 117, 5179.
4. MacKerell, A. D., Jr.; Bashford, D.; Bellot, M.; Dunbrack, R. L., Jr.; Evanseck, J. D.; Field, M. J.; Fischer, S.; Gao, J.; Guo, H.; Ha, S.; Joseph–McCarthy, D.; Kuchnir, L.; Kuczera, K.; Lau, F. T. K.; Mattos, C.; Michnick, S.; Ngo, T.; Nguyen, D. T.; Prodhom, B.; Reiher, W. E., III; Roux, B.; Schlenkrich, M.; Smith, J. C.; Stote, R.; Straub, J.; Watanabe, M.; Wiórkiewicz–Kuczera, J.; Yin, D.; Karplus, M. J Phys Chem B 1998, 102, 3586.
5. Jorgensen, W. L.; Maxwell, D. S.; Tirado–Rives, J. J Am Chem Soc 1996, 118, 11225.
6. van Gunsteren, W. F.; Billeter, S. R.; Eising, A. A.; Hünenberger, P. H.; Krüger, P.; Mark, A. E.; Scott, W. R. P.; Tironi, I. G. Biomolecular Simulation: The GROMOS96 Manual and User Guide; Vdf Hochschulverlag AG an der ETH Zürich: Zürich, 1996.
7. Hagler, A. T.; Ewig, C. S. Comput Phys Commun 1994, 84, 131.
8. Weerasinghe, S.; Smith, P. E. J Chem Phys 2003, 118, 10663.
9. Schuler, L. D.; Daura, X.; van Gunsteren, W. F. J Comput Chem 2001, 22, 1205.
10. Weiner, P. K.; Kollman, P. A. J Comput Chem 1981, 2, 287.
11. Pearlman, D. A.; Case, D. A.; Caldwell, J. W.; Ross, W. S.; Cheatham, T. E., III; DeBolt, S.; Ferguson, D.; Seibel, G.; Kollman, P. A. Comput Phys Comm 1995, 91, 1.
12. MacKerell, A. D., Jr.; Wiórkiewicz-Kuczera, J.; Karplus, M. J Am Chem Soc 1995, 117, 11946.
13. Brooks, B. R.; Bruccoleri, R. E.; Olafson, B. D.; States, D. J.; Swaminathan, S.; Karplus, M. J Comput Chem 1983, 4, 187.
14. Momany, F. A.; Rone, R. J Comput Chem 1992, 13, 888.
15. Nemethy, G.; Gibson, K. D.; Palmer, K. A.; Yoon, C. N.; Paterlini, G.; Zagari, A.; Rumsey, S.; Scheraga, H. A. J Phys Chem 1992, 96, 6472.
16. Levitt, M. J Mol Biol 1983, 168, 595.
17. Levitt, M.; Hirshberg, M.; Sharon, R.; Daggett, V. Comput Phys Comm 1995, 91, 215.
18. van Gunsteren, W. F.; Berendsen, H. J. C. Groningen Molecular Simulation (GROMOS) Library Manual; Biomos: Groningen, 1987.
19. Jorgensen, W. L.; Tirado–Rives, J. J Am Chem Soc 1988, 110, 1657.
20. Hermans, J.; Berendsen, H. J. C.; van Gunsteren, W. F.; Postma, J. P. M. Biopolymers 1984, 23, 1513.
21. Smith, L. J.; Mark, A. E.; Dobson, C. M.; van Gunsteren, W. F. Biochemistry 1995, 34, 10918.
22. Daura, X.; Mark, A. E.; van Gunsteren, W. F. J Comput Chem 1998, 19, 535.
23. van Gunsteren, W. F.; Daura, X.; Mark, A. E. In Encyclopedia of Computational Chemistry; von Ragué Schleyer, P., Ed.; John Wiley & Sons: New York, 1998, p. 1211.
24. Schuler, L. D.; van Gunsteren, W. F. Mol Sim 2000, 25, 301.
25. Chandrasekhar, I.; van Gunsteren, W. F. Curr Sci 2001, 81, 1325.
26. Chandrasekhar, I.; van Gunsteren, W. F. Eur Biophys J 2002, 31, 89.
27. Chandrasekhar, I.; Kastenholz, M. A.; Lins, R. D.; Oostenbrink, C.; Schuler, L. D.; Tieleman, D. P.; van Gunsteren, W. F. Eur Biophys J 2003, 32, 67.
28. Daura, X.; van Gunsteren, W. F.; Rigo, D.; Jaun, B.; Seebach, D. Chem Eur J 1997, 3, 1410.
29. Daura, X.; Gademann, K.; Jaun, B.; Seebach, D.; van Gunsteren, W. F.; Mark, A. E. Angew Chem In Ed 1999, 38, 236.
30. van Gunsteren, W. F.; Bürgi, R.; Peter, C.; Daura, X. Angew Chem In Ed 2001, 40, 351.
31. Daura, X.; Glättli, A.; Gee, P.; Peter, C.; van Gunsteren, W. F. Adv Protein Chem 2002, 62, 341.
32. Bakowies, D.; van Gunsteren, W. F. J Mol Biol 2002, 315, 713.
33. Stocker, U.; van Gunsteren, W. F. Proteins 2000, 40, 145.
34. Stocker, U.; Spiegel, K.; van Gunsteren, W. F. J Biomol NMR 2000, 18, 1.
35. Smith, L. J.; Dobson, C. M.; van Gunsteren, W. F. J Mol Biol 1996, 286, 1567.
36. Smith, L. J.; Dobson, C. M.; van Gunsteren, W. F. Proteins 1999, 36, 77.
37. Antes, I.; Thiel, W.; van Gunsteren, W. F. Eur Biophys J 2002, 31, 504.
38. Oostenbrink, B. C.; Pitera, J. W.; Van Lipzig, M. M. H.; Meerman, J. H. N.; van Gunsteren, W. F. J Med Chem 2000, 43, 4594.
39. Bonvin, A. M.; Sunnerhagen, M.; Otting, G.; van Gunsteren, W. F. J Mol Biol 1998, 282, 859.
40. Czechtizky, W.; Daura, X.; Vasella, A.; van Gunsteren, W. F. Helv Chim Acta 2001, 84, 2132.
41. van Gunsteren, W. F.; Mark, A. E. J Chem Phys 1998, 108, 6109.
42. Berendsen, H. J. C.; Postma, J. P. M.; van Gunsteren, W. F.; Hermans, J. In Intermolecular Forces; Pullman, B. E., Ed.; Reidel: Dordrecht, The Netherlands, 1981, p. 331.
43. Glättli, A.; Daura, X.; van Gunsteren, W. F. J Chem Phys 2002, 116, 9811.
44. Tironi, I. G.; van Gunsteren, W. F. Mol Phys 1994, 83, 381.
45. Walser, R.; Mark, A. E.; van Gunsteren, W. F.; Lauterbach, M.; Wipff, G. J Chem Phys 2000, 112, 10450.
46. Liu, H. Y.; Müller–Plathe, F.; van Gunsteren, W. F. J Am Chem Soc 1995, 117, 4363.
47. Geerke, D. P.; Oostenbrink, C.; van der Vegt, N. F. A.; van Gunsteren, W. F. J Phys Chem B 2004, 108, 1436.
48. Tironi, I. G.; Fontana, P.; van Gunsteren, W. F. Mol Sim 1996, 18, 1.
49. Lins, R. D.; Hünenberger, P. H. Unpublished results.
50. Villa, A.; Mark, A. E. J Comput Chem 2002, 23, 548.
51. Shirts, M. R.; Pitera, J. W.; Swope, W. C.; Pande, V. S. J Chem Phys 2003, 119, 5740.
52. MacCallum, J. L.; Tieleman, D. P. J Comput Chem 2003, 24, 1930.
53. Soares, T.; van Gunsteren, W. F. Unpublished results.
54. Fioroni, M.; Burger, K.; Mark, A. E.; Roccatano, D. J Phys Chem B 2000, 104, 12347.
55. Smith, L. J.; Berendsen, H. J. C.; van Gunsteren, W. F. J Phys Chem A 2004, 108, 1065.
56. Scott, W. R. P.; Hünenberger, P. H.; Tironi, I. G.; Mark, A. E.; Billeter, S. R.; Fennen, J.; Torda, A. E.; Huber, P.; Krüger, P.; van Gunsteren, W. F. J Phys Chem A 1999, 103, 3596.
57. CRC Handbook of Chemistry and Physics: A Ready-Reference Book

of Chemical and Physical Data, 52nd ed.; CRC Press, Inc.: Boca Raton, FL, 1952.
58. van Gunsteren, W. F.; Karplus, M. Biochemistry 1982, 21, 2259.
59. Gurskaya, G. V. The Molecular Structure of Amino Acids. Determination by X-ray Diffraction Analysis; Consultants Bureau: New York, 1968.
60. Tironi, I. G.; Sperb, R.; Smith, P. E.; van Gunsteren, W. F. J Chem Phys 1995, 102, 5451.
61. Radzicka, A.; Wolfenden, R. Biochemistry 1988, 27, 1664.
62. Wolfenden, R. Biochemistry 1981, 20, 849.
63. Ryckaert, J.-P.; Ciccotti, G.; Berendsen, H. J. C. J Comput Phys 1977, 23, 327.
64. Berendsen, H. J. C.; Postma, J. P. M.; Van Gunsteren, W. F.; Dinola, A.; Haak, J. R. J Chem Phys 1984, 81, 3684.
65. Berendsen, H. J. C.; van der Spoel, D.; van Drunen, R. Comput Phys Commun 1995, 91, 43.
66. Lindahl, E.; Hess, B.; van der Spoel, D. J Mol Model 2001, 7, 306.
67. van der Spoel, D.; van Buuren, A. R.; Apol, E.; Meulenhoff, P. J.; Tieleman, D. P.; Sijbers, A. L. T. M.; Hess, B.; Feenstra, K. A.; Lindahl, E.; van Drunen, R.; Berendsen, H. J. C. Gromacs User Manual Version 3.0: Nijenborgh 4, 9747 AG, Groningen, The Netherlands. Internet: http://www.gromacs.org, 2001.
68. Heinz, T. N.; van Gunsteren, W. F.; Hünenberger, P. H. J Chem Phys 2001, 115, 1125.
69. Beveridge, D. L.; DiCapua, F. M. Annu Rev Biophys Biophys Chem 1989, 18, 431.
70. Beutler, T. C.; Mark, A. E.; Van Schaik, R. C.; Gerber, P. R.; van Gunsteren, W. F. Chem Phys Lett 1994, 222, 529.
71. Njo, S. L.; van Gunsteren, W. F.; Müller–Plathe, F. J Chem Phys 1995, 102, 6199.
72. Norrby, P. O.; Liljefors, T. J Comput Chem 1998, 19, 1146.
73. Faller, R.; Schmitz, H.; Biermann, O.; Müller–Plathe, F. J Comput Chem 1999, 20, 1009.
74. Riddick, J. A.; Bunger, W. B.; Sakano, T. K. Organic Solvents, Physical Properties and Methods of Purification; John Wiley & Sons: New York, 1986.
75. Majer, V.; Svoboda, V. Enthalpies of Vaporization of Organic Compounds: A Critical Review and Data Compilation; Blackwell Scientific Publications: Oxford, 1985.
76. Nilsson, S.-O.; Wadsö, I. J Chem Thermodyn 1986, 18, 673.
77. CRC Handbook of Chemistry and Physics: A Ready-Reference Book of Chemical and Physical Data; CRC Press, Inc.: Boca Raton, FL, 2000.
78. Haines, W. E.; Helm, R. V.; Bailey, C. W.; Ball, J. S. J Phys Chem 1954, 58, 270.
79. Haines, W. E.; Helm, R. V.; Cook, G. L.; Ball, J. S. J Phys Chem 1956, 60, 549.
80. Scott, D. W.; Finke, H. L.; Hubbard, W. N.; McCullough, J. P.; Oliver, G. D.; Gross, M. E.; Katz, C.; Williamson, K. D.; Waddington, G.; Huffmann, H. M. J Am Chem Soc 1951, 74, 4656.
81. Wagman, P. D.; Evans, W. H.; Parker, V. B.; Schumm, R. H.; Halow, I.; Bailey, S. M.; Churney, K. L.; Nuttall, R. L. J Phys Chem Ref Data 1982, 11, 1.
82. Guillot, B. J Mol Liq 2002, 101, 219.
83. Price, D. J.; Brooks, C. L., III. J Comput Chem 2002, 23, 1045.
84. Bash, P. A.; Singh, U. C.; Langridge, R.; Kollman, P. A. Science 1987, 236, 564.
85. Jorgensen, W. L.; Briggs, J. M.; Contreras, M. L. J Phys Chem 1990, 94, 1683.
86. Schäfer, H.; van Gunsteren, W. F.; Mark, A. E. J Comput Chem 1999, 20, 1604.
87. Wescott, J. T.; Fisher, L. R.; Hanna, S. J Chem Phys 2002, 116, 2361.
88. Mu, Y.; Stock, G. J Phys Chem B 2002, 106, 5294.
89. Hu, H.; Elstner, M.; Hermans, J. Proteins 2003, 50, 451.
90. Mu, Y.; Kosov, D. S.; Stock, G. J Phys Chem B 2003, 107, 5064.
91. Yu, H. B.; Hansson, T.; van Gunsteren, W. F. J Chem Phys 2003, 118, 221.
92. Berendsen, H. J. C.; Grigera, J. R.; Straatsma, T. P. J Phys Chem 1987, 91, 6269.